

Sea level controls on the textural characteristics and depositional architecture of the Hueneme and associated submarine fan systems, Santa Monica Basin, California

W.R. NORMARK*, D.J.W. PIPER[†] and R.N. HISCOTT[‡]

*U.S. Geological Survey, MS-999, 345 Middlefield Road, Menlo Park, California 94025, USA, [†]Atlantic Geoscience Centre, Geological Survey of Canada (Atlantic), P.O. Box 1006, Dartmouth, Nova Scotia, B2Y 4A2, Canada, [‡]Earth Sciences Department, Memorial University of Newfoundland, St. John's, Newfoundland, A1B 3X5, Canada

ABSTRACT

Hueneme and Dume submarine fans in Santa Monica Basin consist of sandy channel and muddy levee facies on the upper fan, lenticular sand sheets on the middle fan, and thinly bedded turbidite and hemipelagic facies elsewhere. Fifteen widely correlatable key seismic reflections in high-resolution airgun and deep-towed boomer profiles subdivide the fan and basin deposits into time-slices that show different thickness and seismic-facies distributions, inferred to result from changes in Quaternary sea level and sediment supply. At times of low sea level, highly efficient turbidity currents generated by hyperpycnal flows or sediment failures at river deltas carry sand well out onto the middle-fan area. Thick, muddy flows formed rapidly prograding high levees mainly on the western (right-hand) side of three valleys that fed Hueneme fan at different times; the most recently active of the lowstand fan valleys, Hueneme fan valley, now heads in Hueneme Canyon. At times of high sea level, fans receive sand from submarine canyons that intercept littoral-drift cells and mixed sediment from earthquake-triggered slumps. Turbidity currents are confined to 'underfit' talweg channels in fan valleys and to steep, small, basin-margin fans like Dume fan. Mud is effectively separated from sand at high sea level and moves basinward across the shelf in plumes and in storm-generated lutite flows, contributing to a basin-floor blanket that is locally thicker than contemporary fan deposits and that *onlaps* older fans at the basin margin. The infilling of Santa Monica Basin has involved both fan and basin-floor aggradation accompanied by landward and basinward facies shifts. Progradation was restricted to the downslope growth of high muddy levees and the periodic basinward advance of the toe of the steeper and sandier Dume fan. Although the region is tectonically active, major sedimentation changes can be related to eustatic sea-level changes. The primary controls on facies shifts and fan growth appear to be an interplay of texture of source sediment, the efficiency with which turbidity currents transport sand, and the effects of delta distributary switching, all of which reflect sea-level changes.

INTRODUCTION

The problem

Studies of ancient turbidite sequences have suggested that there is an important relationship

between sea-level change and the deposition of basinal sands (e.g. Posamentier *et al.*, 1988; Mutti, 1985, 1992). Most of the studies of modern deep-sea fans where acoustic facies can be correlated with dates from long sediment cores, are from

larger deep-water muddy fans such as the Amazon and Mississippi fans, even though small sandy fans, developed on shallower continental crust, are easier to survey and are of greater interest because they represent more important hydrocarbon-reservoir analogues. This imbalance in fan studies stems from major problems in acoustically imaging and sampling the medium to thickly bedded sand and gravel on the small fans, in resolving the small morphological elements of such fans, and in positioning sampling instruments within the elements (e.g., Normark *et al.*, 1979, 1993).

We chose Hueneme fan, in the California Continental Borderland, as an example of a small sandy fan where we could study the effect of late Quaternary sea-level change on a submarine fan system. The relatively shallow setting of Hueneme fan allowed us to resolve the important stratal surfaces and thickness of sand units by integrating high-resolution single-channel airgun data (this paper) with even higher resolution, but lower penetration, deep-towed boomer records (Piper *et al.*, 1994).

The location

Hueneme fan is the largest of a series of sandy submarine fans filling the Santa Monica Basin west of Los Angeles, California (Fig. 1). A number of submarine canyons at present cross the narrow continental shelf, intercepting littoral sediment transport and redirecting the sediment onto Hueneme, Mugu, Dume, Santa Monica and Redondo fans. The basin appears to have been a relatively stable depocentre since the Pliocene (Vedder, 1987; Teng & Gorsline, 1989). Santa Monica Basin is bounded by oblique-slip faults in a transpressive regime with relatively little deformation of the basin floor (Crouch & Suppe, 1993; Klitgord & Brocher, 1996). Related folding has produced a growing anticline along the eastern margin of Santa Monica Basin, across lower Santa Monica canyon. Dahlen *et al.* (1990) have defined tectonic tilting of the continental shelf near Hueneme canyon from NW to SE. Santa Monica Basin reaches a maximum water depth of just shallower than 1000 m. This relatively shallow water depth, compared with most deep-sea fans, allowed good spatial resolution of stratigraphic

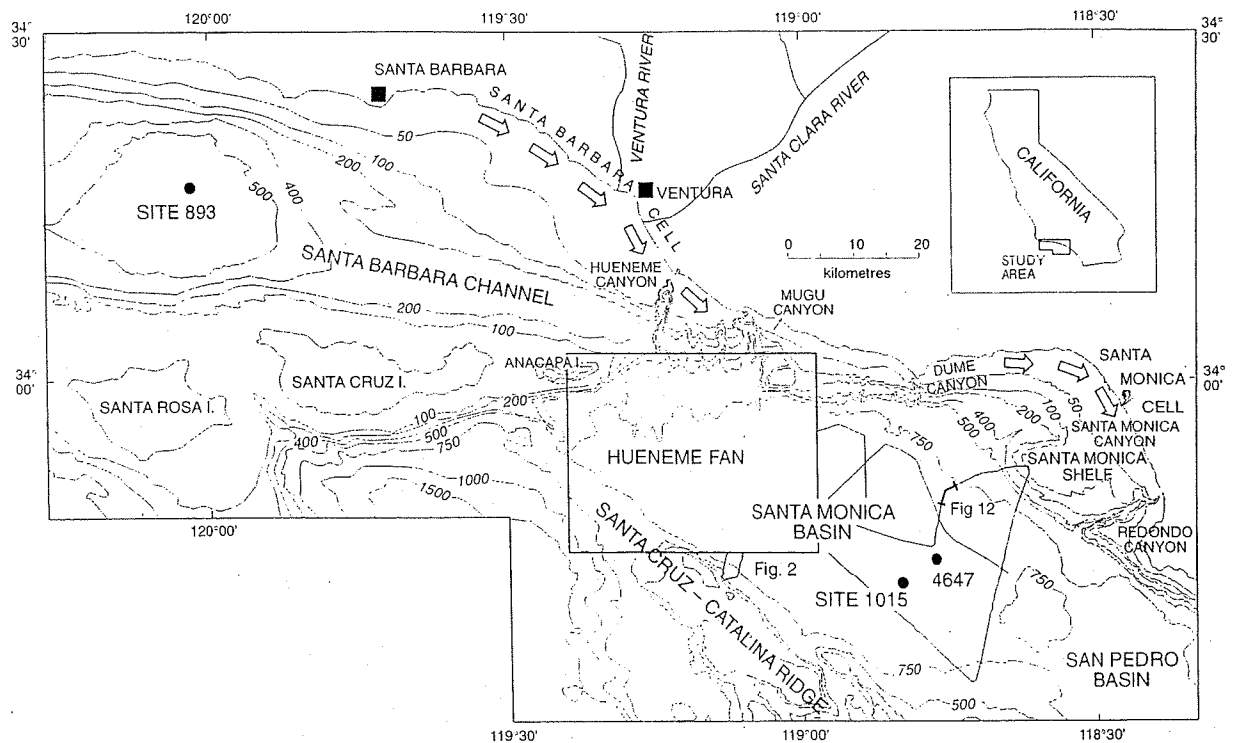


Fig. 1. Location map showing regional setting and bathymetry of Hueneme fan, Santa Monica Basin. Contours in metres. Littoral cells after Nardin (1981). Solid circles denote dated sediment core localities: 4647 is a piston core of Emery and Bray (1962), Site 893 was cored to 196.5 metres on ODP Leg 146 (Shorebased Scientific Party, 1994) and Site 1015 was cored to 150 metres on ODP Leg 167 (Shipboard Scientific Party, 1997). Box shows location of Fig. 2. Survey tracks are only shown where they extend outside the Fig. 2 box. See Fig. 2 for other survey tracks.

units from seismic-reflection profiling systems towed near the sea surface.

The narrow continental shelf off southern California receives sediment from small ephemeral rivers (Schwalbach & Gorsline, 1985). Sand is transported southeastward in longshore currents until it is intercepted by a submarine canyon at the downdrift end of a littoral cell. Mud on the shelf is periodically resuspended by storm waves and advected southeastward in the prevailing current and seaward into the basins (Thornton, 1984). Hueneme Canyon is the first canyon at the eastern end of the long Santa Barbara littoral cell (Fig. 1); the canyons to the southeast are fed by much shorter littoral cells. At lowstands of sea level, the littoral cell on the north side of Santa Barbara Basin was inactive and Hueneme Canyon was fed directly by the Santa Clara River (Fig. 9 of Behl, 1995; Dahlen *et al.*, 1990).

Sand is transported into Santa Monica Basin by turbidity currents flowing down the shelf-edge canyons. Some mud is also transported by turbidity currents, some by episodic high-concentration storm advection, and some by 'background' hemipelagic processes (Thornton, 1984). Slope failures locally occur on steep basin margins away from the canyons. At present, little sediment, coarse or fine, is deposited on the continental shelf, which is a zone of sediment bypassing, but significant trapping of sediment on the shelf occurred during the earliest stages of the Holocene marine transgression (Nardin, 1983).

Pollen data from Site 893 indicates that during glacial maxima, the coastal areas adjacent to Santa Barbara Basin received higher precipitation, perhaps in the range of 600–1000 mm compared with ≈ 400 mm at present, but conditions were still essentially arid (Heusser, 1995). Total sediment delivery by rivers was thus likely higher during glacial periods. Modern sediment discharge from the Santa Clara River (Milliman & Syvitski, 1992) makes it a river with high sediment concentration likely to produce hyperpycnal flows during major floods (Mulder & Syvitski, 1995).

Previous work

The deeper seismic-stratigraphic architecture of Santa Monica Basin has been described by Teng and Gorsline (1989) and Crouch and Suppe (1993). The southwestern margin of the basin along the Santa Cruz–Catalina Ridge (Fig. 1) is marked by a major strike-slip fault. The north-

eastern margin of the basin against the continental slope is also bounded by faults forming part of a broad anticlinal structure.

The previous detailed study of the area, by Nardin (1981, 1983), concluded that, 'in general, large-scale fan growth fits Normark's model in which the suprafan is the primary locus of coarse sediment deposition'. Nardin also demonstrated an impact of changing sea level on the Santa Monica Basin fans, with a decrease in the areal extent of fan sedimentation between 18 ka and 10 ka during the rise in sea level from isotopic Stage 2 to Stage 1, when sediment was trapped on the narrow shelves. Nardin's interpretation was based on a grid of 3.5 kHz seismic-reflection profiles at 5–10 km spacing on the fan and a few 10 cu-inch (164 cm^3) airgun profiles spaced at ≈ 15 km, in addition to some deeper penetration seismic-reflection data. Location of the seismic-reflection data is shown by Teng and Gorsline (1989, their Figs 2–4). Subsequently, GLORIA long-range sidescan-sonar data were obtained from Santa Monica Basin (EEZ-Scan 84 Scientific Staff, 1986); these data have recently been interpreted by Edwards *et al.* (1996) in conjunction with available samples and high-resolution seismic-reflection profiles. Large numbers of box cores and fewer short piston cores are available from the basin (e.g. Gorsline & Emery, 1959; Reynolds, 1987; Edwards *et al.*, 1996).

Nardin (1981, 1983) applied sequence analysis to his seismic-reflection profiles and defined two mid to upper Quaternary units (C and D in his nomenclature) inferred to have been deposited since 0.5 Ma. He noted that Dume fan was active during accumulation of sequence C, but has been overlapped by later basin plain sediments (90 m thick, sequence D). He also recognised an '8-m reflector' at a sub-bottom depth of 8 m in southeastern Santa Monica Basin that piston cores indicate corresponds approximately to the base of the Holocene at 10 ka. He was unable to trace this reflector onto Hueneme and Mugu fans. Dahlen *et al.* (1990) show that the steep slopes between the shelf and basin, with common onlapping reflectors, preclude tracing of acoustic horizons from the basin to the shelf, thus further limiting basin-wide stratigraphic interpretation.

Bathymetry and fan divisions

Santa Monica Basin reaches a maximum depth of 938 m in the ponded southern part, rising gently to the northwest to Hueneme fan, which forms a pronounced bathymetric lobe at 750–850 m

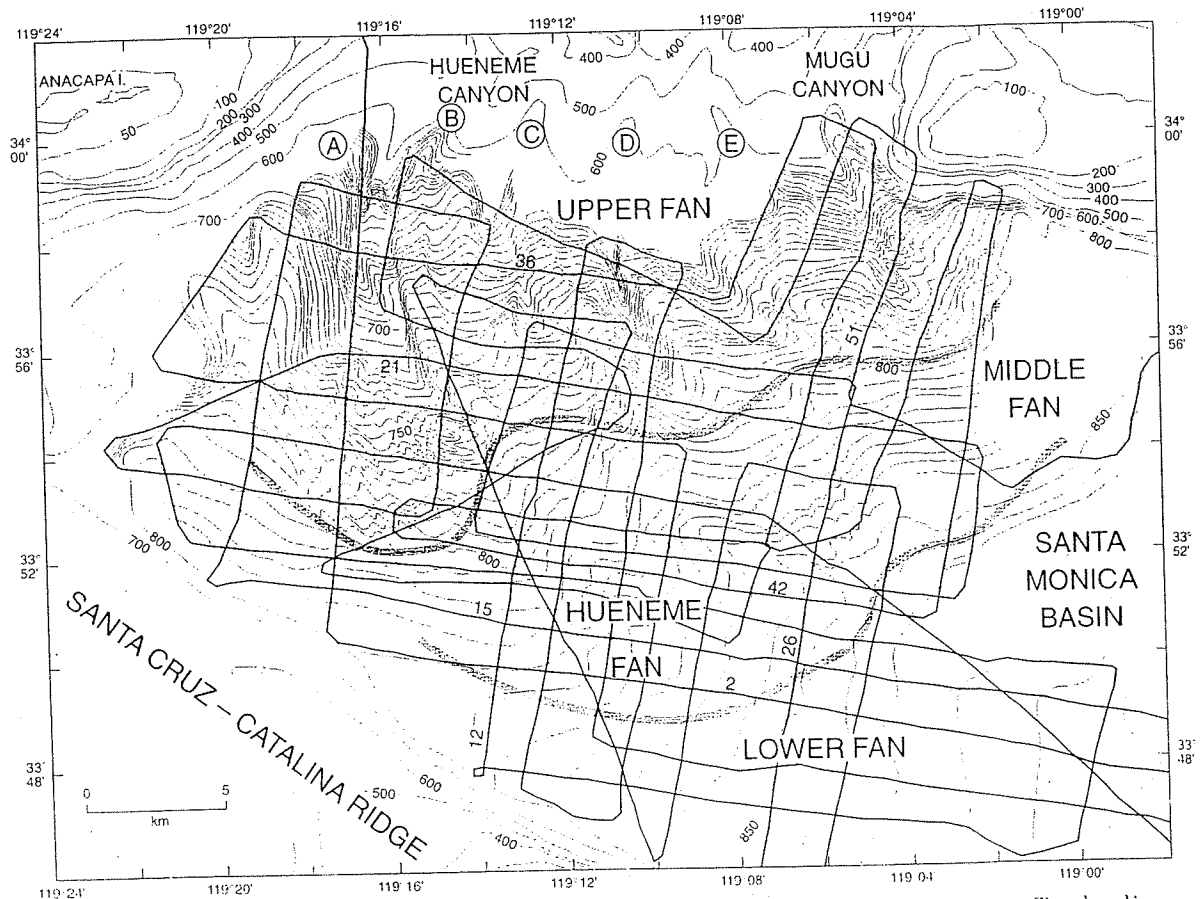


Fig. 2. Bathymetry of Hueneme fan showing seismic-reflection track lines. Contours in metres. Tracks discussed in the text are numbered. (A) to (E) are valleys discussed in text. Broad lines mark subdivisions of the fan. Staircase contour lines at $119^{\circ}16'$ to $18' W$ mark sediment waves on the upper fan, but are highly schematic. (Bathymetry after Piper *et al.*, 1994).

(Fig. 2). Hueneme fan valley has a distinct bathymetric expression to about 780 m water depth.

Hueneme, Mugu, Dume and Redondo canyons are all incised into the shelf and head near the present coastline; Santa Monica Canyon has not eroded across the shelf. Redondo Canyon at present leads to San Pedro Basin, not to Santa Monica Basin. There is a series of prominent slope gullies between Hueneme and Mugu canyons.

The division of the submarine fan deposits in western Santa Monica Basin into upper, middle and lower fan components is complicated by the fact that there have been several canyons and upperfan valleys active at different times during the Quaternary (see below). Five main morphological valleys extend across the upper fan surface: Hueneme (= B), (C), (D), (E) and Mugu (Fig. 2), as well as an additional depression along the western margin of the fan (shown as (A), Fig. 2). We therefore recognise a composite upper fan that includes deposits from all of these valleys and their associated prominent levees. The tran-

sition to the middle fan is placed where levee relief becomes subdued (Fig. 2). The middle fan has a convex-upward shape, is crossed by several low-relief valleys, and is underlain by acoustically reflective and hummocky deposits that are interpreted as sand lenses and irregular sand sheets on deep-tow boomer profiles (Piper *et al.*, 1994). The lower fan extends from the distal limit of these interpreted sand deposits at a depth of ≈ 850 m to the flat central basin floor.

DESCRIPTION OF THE SEISMIC STRATIGRAPHY

Methods

Collection of the seismic-reflection data for this study utilized three systems with different reflector resolution and acoustic penetration capabilities. Trackline grid spacings were 0.5–3 km over Hueneme fan (Fig. 2), which is the main focus of this paper. For conventional seismic-reflection

profiling, a Texas Instruments 40 cu-in (650 cm³) sleeve gun, run at 1300 psi, was fired every 3 s. Signals were detected on a Seismic Engineering (SE) 30-m hydrophone array and a Nova Scotia Research Foundation (NSRF) Mark 5a 6-m hydrophone array. (These acronyms are used throughout the paper to specify types of seismic profiles). The 30-m SE streamer provided good data typically to depths of 1.2 s with reflector resolution of about 50 ms roundtrip travel (≈ 35 m) (Fig. 3a). The NSRF array obtained useful data to ≈ 0.4 s but with a higher frequency bandwidth that provided resolution of about 30 ms (≈ 20 m) (Fig. 3b). In addition, a high-resolution Hunttec boomer system towed several hundred metres below the sea surface (about half the water depth) was used to image the upper few tens of milliseconds with a resolution of better than 0.5 ms (0.4 m) (Fig. 3c–e). The survey tracklines are accurate to ± 30 m based on GPS data.

Stratigraphic marker horizons

Key seismic-marker horizons were distinguished at changes in acoustic facies or local unconformities within the basin, and most are defined at the intersection of lines 12 and 15 (Figs 2 and 4). Reflections A, B and C were defined on the SE 30-m profiles (Figs 3a and 4). In many areas, reflection C was also clearly traceable on the NSRF records, on which overlying regional reflections D, F and J were also distinguished (Figs 3b and 5). Locally, away from the intersection of lines 12 and 15, intermediate reflections E, G, H, I and K were distinguished on the NSRF records (Fig. 5).

Key reflections L, M, N and O, in the upper 25 ms of sediment, were defined using boomer records for Hueneme fan east of Hueneme channel (Fig. 3c–e). These key reflections can only be correlated approximately with the basin-floor area. Detailed results of this high-resolution study will be reported in a recently submitted companion paper, but the data are used in places in this study to validate correlations. Where possible, seismic reflections A through O were traced throughout the survey grid (Fig. 2). Correlations were checked at each trackline intersection to ensure precise tracing.

Seismic facies

Five principal seismic facies are distinguished in NSRF sleeve-gun records, on the basis of reflection amplitude, continuity and geometry. Lithologic interpretations of these seismic facies can be

made from their geometry, comparison with facies in boomer profiles, and their near-surface distribution compared with cores described by Gorsline and Emery (1959) and Edwards *et al.* (1996). The *channel facies* consists of discontinuous, irregular, high-amplitude reflections that tend to fill depressions and are commonly bounded by levees (line 36, Figs 3b and 5). The *high-levée facies* has low amplitude, continuous reflections that appear acoustically transparent where more steeply dipping and has the overall linear mounded form of a levee (line 36, Figs 3b and 5). The high levees pass laterally into the *low levee-prodelta facies* (not distinguished in Fig. 5), which shows little relief and consists of relatively low-amplitude continuous reflections. This facies occurs on the continental slope around Hueneme fan and on levee flanks adjacent to the high levee facies. The *sandy-sheet facies* is highly reflective with moderately continuous, moderate-amplitude reflections commonly defining a lenticular geometry with downlap reflection terminations (line 42, Fig. 5). The *lower-fan facies* is widespread on the floor of Santa Monica Basin and the lower part of Hueneme fan. It consists of subparallel medium-to high-amplitude reflections that commonly show onlap terminations at basin margins and on lower Hueneme and Dume fans (Figs 6 and 7).

Depositional history of Hueneme fan and the adjacent basin

The correlation of key reflectors throughout Santa Monica Basin and within Hueneme and Dume fans, shown schematically in Fig. 8, allows the sequential growth of the deep-sea fans to be determined. Except at the basin margin, reflection A is not cut by faults and forms a reasonably flat horizon over most of the basin (Figs 4 and 8). The sequence between A and B appears generally ponded and resulted in a reduction of basin-floor relief within the deeper part of the basin. Overlying sediment of Hueneme fan thins from the upper fan to the basin plain and key reflections become more regular downfan (Figs 4 and 5). The distribution and thickness of seismic facies suggest that most sediment reaching the basin has been transported across Hueneme fan from entry points between Hueneme and Mugu Canyons. Because seismic resolution decreases downsection, we describe fan development from the seafloor downward.

Transport of near-surface sediment (above reflector K) has been down Hueneme Canyon (Figs 3b, 5a). On the upper fan, this resulted in

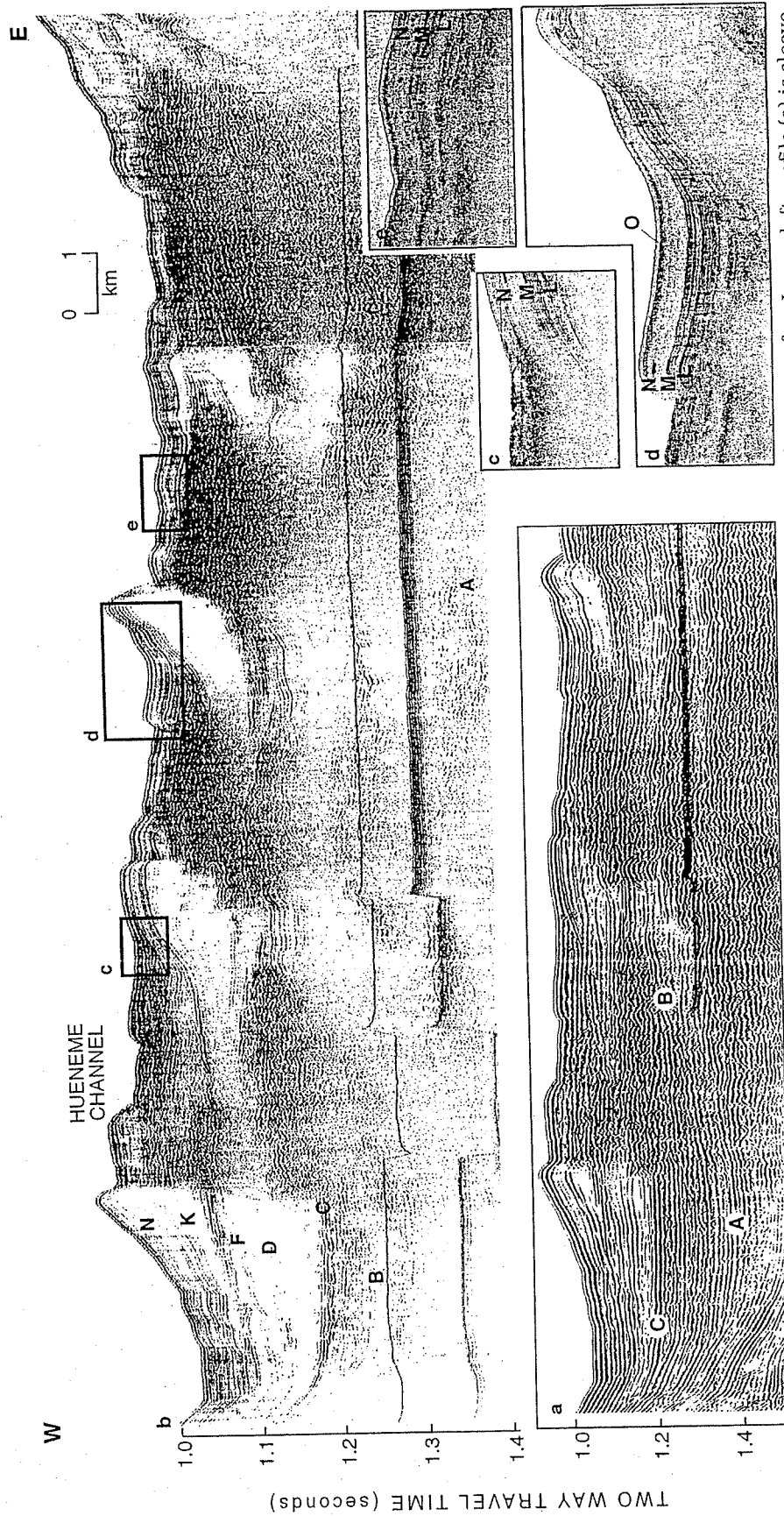


Fig. 3. Seismic-reflection profiles of varying resolution (see text) along strike line 36 across the upper part of Hueneeme fan. Lower left profile (a) is sleeve-gun record with 30-m SE streamer (vertical exaggeration (v.e.) about x4.5). Upper profile (b) is corresponding sleeve-gun record with NSRF eel (v.e. about x9); facies interpretation in Fig. 5). Insets (c) to (e) are selected segments of boomer records located on the upper NSRF record, with v.e. about x20. A to O are key reflections that are correlatable locally (L-O) or over much of the fan and basin (A-K).

the formation of a high, muddy western levee to the broad channel (Fig. 3a,b). Later, channel width was reduced and an inner sand-mud levee was deposited between the channel axis and the main levee crest (Fig. 3b,c). Extensive sheet-sand bodies were deposited on the middle fan (Figs 5 and 9). Sediment above reflector L on the basin plain onlaps the distal margin of the fan (Fig. 9).

Around reflector J time, Hueneme Canyon, Mugu Canyon and two intervening valleys (C) and (D) (Fig. 5) appear to have been active conduits for coarse sediment at different times (Figs 3a, b and 9). The greatest thicknesses of sediment were deposited on the western (right hand) levee of the Hueneme Canyon system (Fig. 10a), principally between reflectors J and N, with the development of sediment waves (Fig. 2). Between reflectors F and J, channel (C) (later) and channel (D) (earlier) appear to have been the principal sediment conduits and each built a high-relief western levee. Lenticular sheet sands were deposited on the middle fan, with greatest sand thickness directly downfan from the dominant channel. This is illustrated by the shift in sand depocentres on line 42 (Fig. 5) from G and H → J → surface lobe as activity shifted westward from channel (D) → (C) → (B = Hueneme) as depicted in line 36 (Fig. 5).

Between reflectors C and F time, Hueneme Canyon was the dominant conduit, with some sediment supply through Mugu Canyon (Fig. 9). A prominent levee developed west of the ancestral Hueneme fan valley. The substantial thickening above reflector D is consistent with the facies map (Fig. 9, reflector B time) that shows only middle and lower fan deposits in our seismic-reflection profiles before this time. Nevertheless, the sandy sheet facies appears less extensive at reflector D time than at higher levels in the stratigraphic sequence.

Below reflector C, some channels are visible in the western part of Hueneme fan (Figs 5 and 8). Basinal sediment thickness between C and A is greater than sediment thickness on the fan (e.g., line 21, Fig. 5), a condition similar to that above reflector K. The principal depocentre was south-east of the present Hueneme Canyon (Fig. 10).

Depositional history of Dume fan

The growth pattern of Dume fan is more difficult to discern because coarse units are closely stacked one on another and interbedded well-stratified units are not thick enough to present a clear acoustic signature on sleeve-gun seismic-

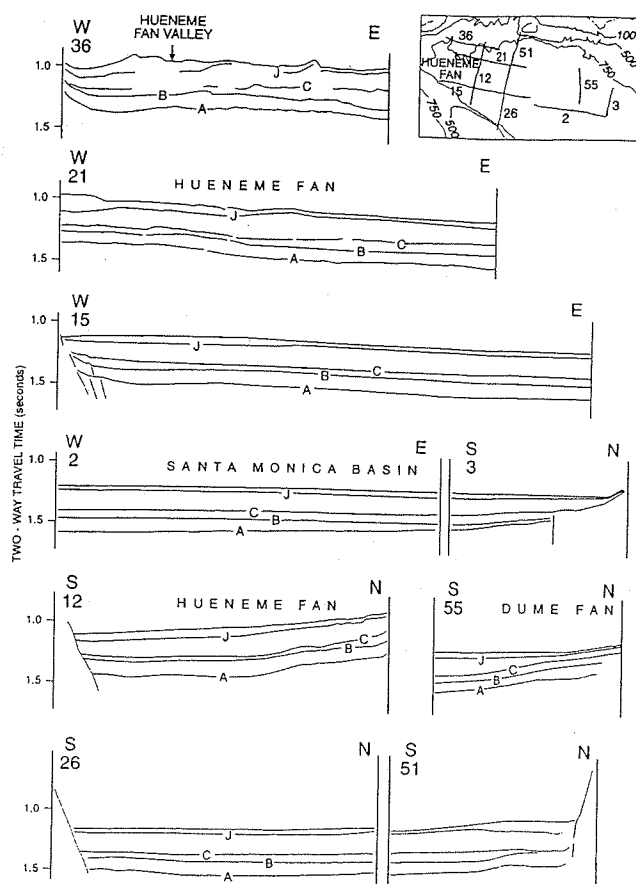


Fig. 4. Basin framework illustrated in a series of line drawings of key sleeve-gun records with 30-m SE streamer across Hueneme fan and Santa Monica Basin, showing the A, B, C and J correlatable reflections through key tracklines shown on inset.

reflection profiles. There is substantial onlap at the margin of the fan that does not appear precisely synchronous on adjacent radial profiles of the fan (Fig. 6). This might result from distributary shifting, because the development of progradation rather than onlap depends in part on the position of the fan distributary. The boomer records (e.g., Fig. 11) provide insight into the interpretation of the lower-resolution sleeve-gun records. Sediment above reflector N is relatively transparent and well-stratified. Just below reflector N, a distinctive surface with hyperbolic reflecting character has been imaged only on the fan itself. This acoustic response is similar to that generated by deep-sea channel gravel waves (e.g., Piper & Savoye, 1993). Between reflectors K and N, there are at least two wedge-like pinch-outs of coarse sediment at the basin margin and there is a thicker pinch-out between reflectors J and K. Deeper pinch-outs are interpreted from sleeve-gun data near reflectors H and C and at a level near

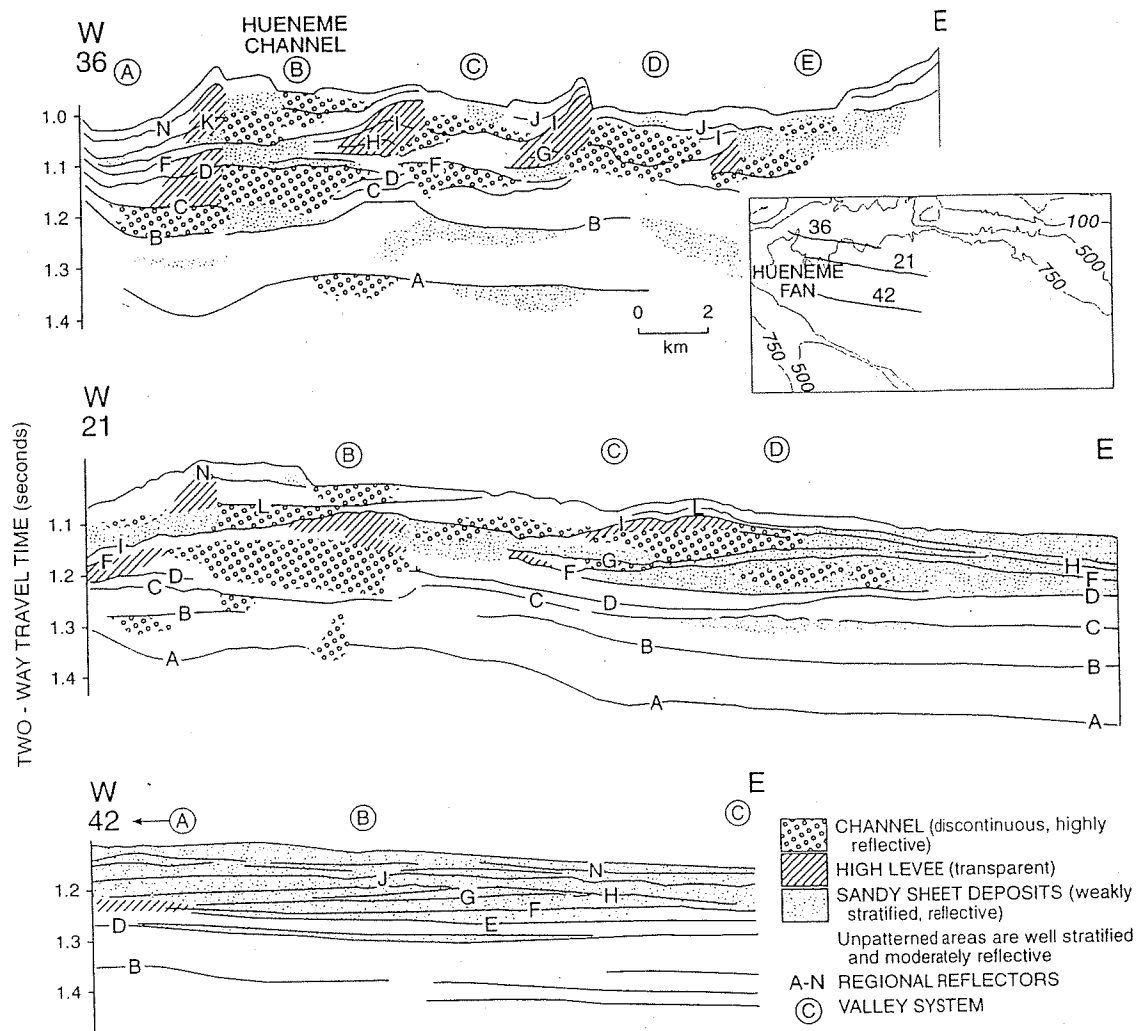


Fig. 5. Facies interpretation from three strike lines across Hueneme fan, run with sleeve gun using NSRF eel. Line 36 (cf. Fig. 3b); line 21 (cf. Fig. 4); line 42 (cf. Fig. 7). Note that reliability of facies interpretation decreases with increasing depth subbottom. Refer to Fig. 2 for canyon/valley locations, e.g. (A).

reflector A (Fig. 6). These pinch-outs represent successive progradational episodes bounded by onlapping basin-floor deposits. The basin-floor sediments were likely derived from the Hueneme fan system to the west of Dume fan (Fig. 1).

CHRONOLOGY

Dated cores

Emery and Bray (1962) reported ^{14}C dates at 3.9 m below sea floor (mbsf) from a piston core (4647; Fig. 1) in southern Santa Monica Basin. Two age determinations gave 4.9 ka on organic carbon and 6.2 ka on carbonate. Nardin (1981) extrapolated this data to suggest that the 8-m reflector (our reflector N) has an age of about 10 ka. This is consistent with extrapolation of late Holocene

sedimentation rates derived from ^{210}Pb chronology (Malouta *et al.*, 1981; Christensen *et al.* 1994). However, Emery and Bray's data are quite variable and in nearby open-barrel cores the obtained ages of 5.8 ka at 1.4 mbsf and 3.6 ka at 0.15 mbsf. A longer chronology is provided by ODP Site 1015 in southeastern Santa Monica Basin (Fig. 1), which penetrated 150 m recovering sediments < 60 ka at the bottom of the hole (Shipboard Scientific Party, 1997).

Hemipelagic sequences at basin margins

Seismic-reflection sections at the basin margin (e.g. extreme western end of line 36 in Fig. 3 Fig. 12) show alternations of well-stratified, high amplitude reflections and more transparent intervals. Only a few key reflections can be correlated from the basin floor to the basin margin

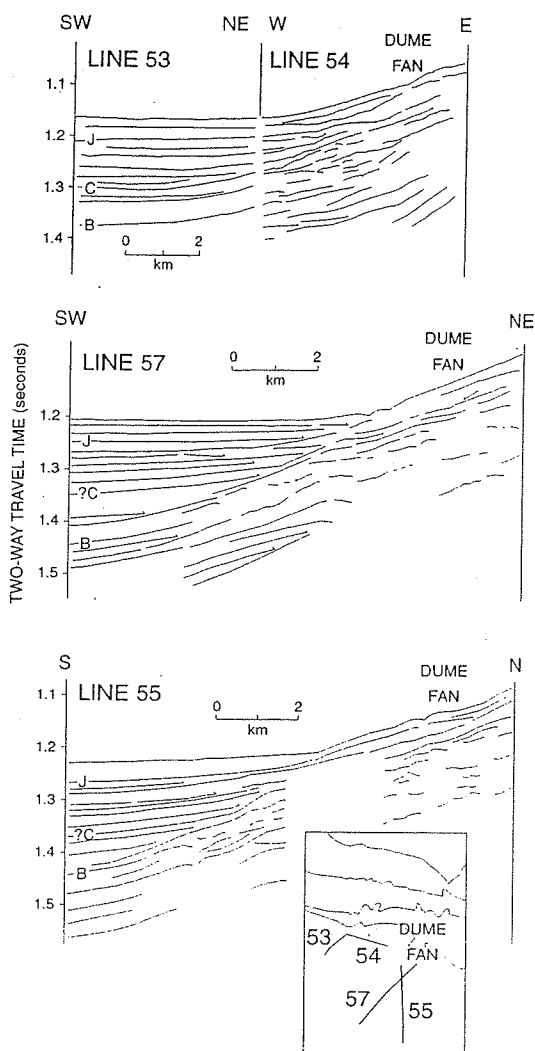


Fig. 6. Line drawings of three sleeve gun records with NSRF eel showing key reflections and interpretation of onlap surfaces (small arrow symbol) on Dume fan.

(Figs 8 and 12) and distinction of acoustic character is more difficult deeper in the section. In general, near-surface sediment is relatively transparent, but a well-stratified interval is found between reflections J and K, overlying another thin, relatively transparent interval. A thicker stratified interval overlies reflection C (Fig. 12). Below C is a relatively transparent interval overlying a more stratified interval that corresponds to the interval around the A reflection within the basin. Changes in reflectivity on the basin margins above the depositional reach of basal turbidity currents may well correlate with shifts in former river mouth positions and changes in the dispersal of hemipelagic silt. The transparent interval above K on the Santa Monica margin (Fig. 12) may correspond to the reduction in stream gradients associated with the late-glacial rise in sea level and the trapping of silt on the shelf.

Comparison with Santa Barbara Basin

ODP Site 893 penetrated a muddy, predominantly hemipelagic sequence in central Santa Barbara Basin, about 10 km from the shelf break (Fig. 1; Shorebased Scientific Party, 1994). To a first approximation, hemipelagic sections around the margin of the Santa Monica Basin would be expected to have a similar sedimentation rate (e.g. Schwabach & Gorsline, 1985). The base of Site 893, at 200 mbsf, is within isotopic Stage 6 (Fig. 8). Precise oxygen isotope stratigraphy suggests the last interglacial (125 ka) at 147 mbsf, isotopic Stage 4 (65 ka) at 86 mbsf, and the last glacial maximum (18 ka) at 29 mbsf (Kennett, 1995).

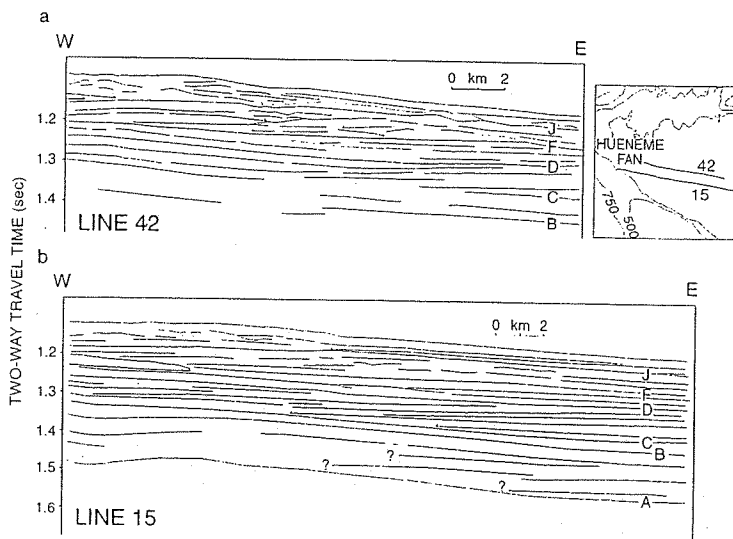


Fig. 7. Line drawings from seismic-reflection lines 42 and 15, using sleeve gun and NSRF eel, showing key reflections and interpretation of onlap surfaces (small arrow symbol). (a) Line 42 on middle Hueneme fan. (b) Line 15 on the proximal basin plain. Stipple indicates distal end of transparent section of levee facies. Profiles located on Fig. 2.

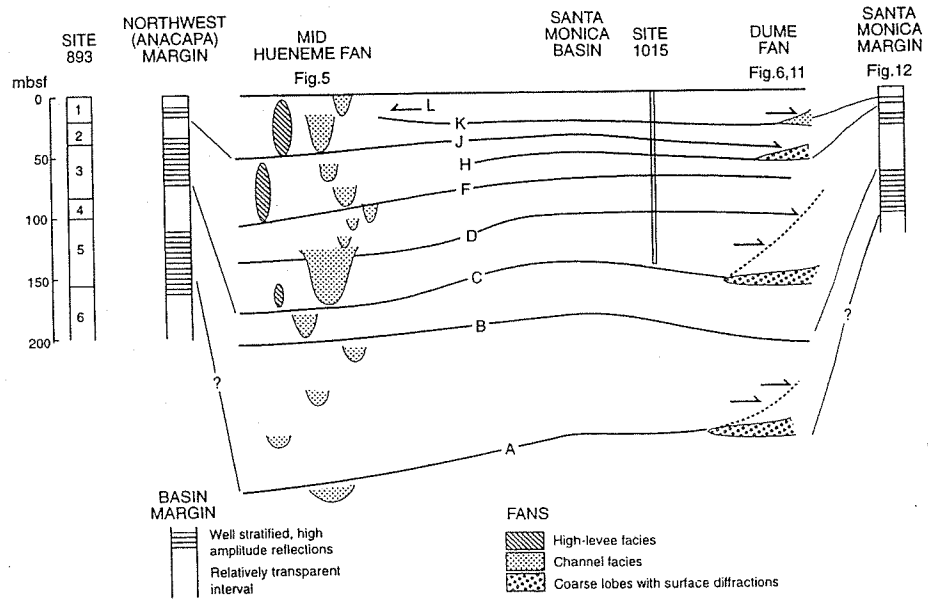


Fig. 8. Schematic summary of seismic-stratigraphic nomenclature, variation in thickness and distribution of major architectural elements for Hueneme and Dume fans and Santa Monica Basin, and correlation with basin-margin sediments. For comparison, stratigraphic thicknesses of isotopic stages in Santa Barbara Basin (ODP Site 893; Shorebased Scientific Party, 1994: Fig. 1) are shown. Channel widths and depths are drawn to reflect actual dimensions. Also shows approximate stratigraphic position of ODP Site 1015 (Shipboard Scientific Party, 1997).

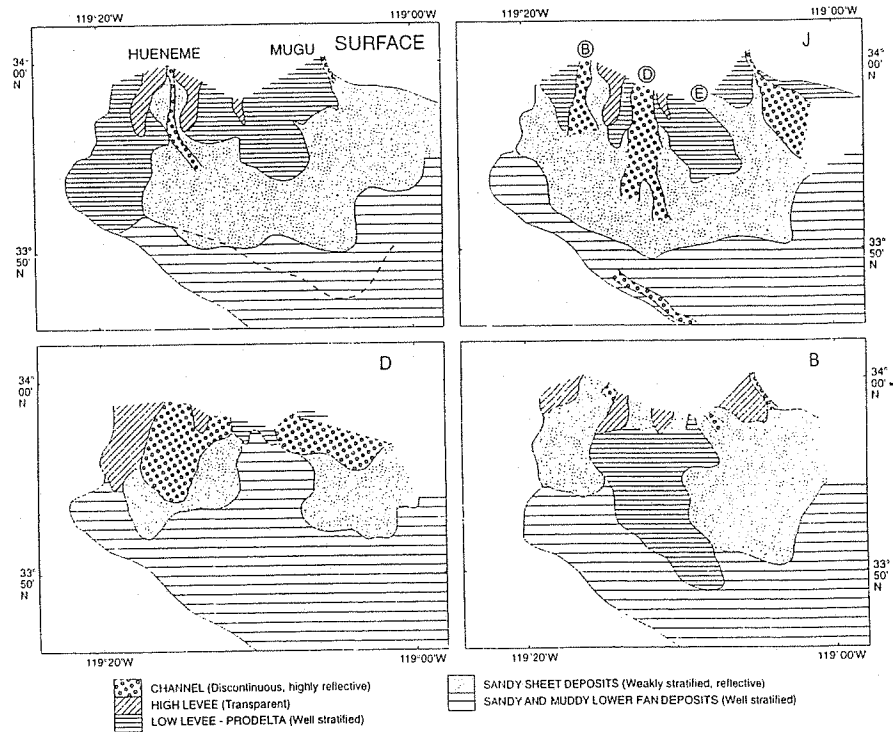


Fig. 9. Palaeo-facies maps based on seismic-reflection character in sleeve gun records with NSRF eel at four stratigraphic levels: near surface and immediately above reflectors, J, D and B. (Dashed line shows onlap of reflector L on reflector K).

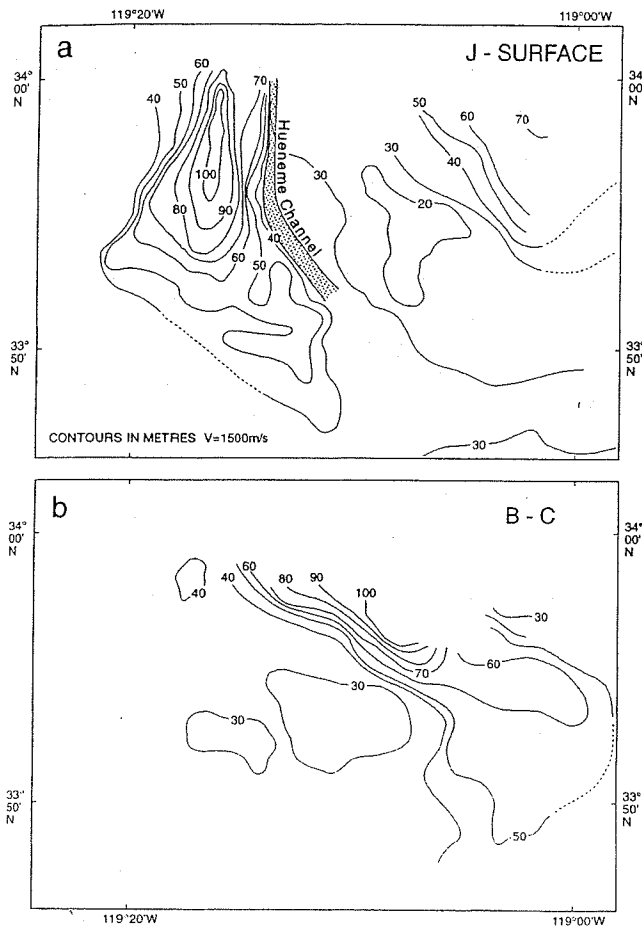


Fig. 10. Isopach maps of selected sediment intervals in Santa Monica Basin. (a) Surface to J; (b) B to C. Compare palaeo-facies maps for the base of these intervals (Fig. 9). Modern Hueneme Channel floor shown for comparison.

DISCUSSION AND SYNTHESIS

Chronology

The various lines of evidence for the chronology reviewed above suggest that the last glacial maximum lowstand of sea level (isotopic Stage 2) corresponds to somewhere around reflector J. This is an interval of silty hemipelagic sedimentation on the basin margin (Fig. 13), wide turbidity-current channels with high, muddy levees on upper Hueneme fan, and coarse-sediment lobes on Dume fan (Fig. 8). Using these characteristics as a guide, the intervals between C and D, and around A, are interpreted as lowstand deposits.

Boomer records show that Holocene sediment accumulation, above reflector N, is thickest on the deeper Santa Monica Basin floor, onlaps at basin margins and on Dume and Hueneme fans, forms a

thin drape over Hueneme fan, and a thin acoustically transparent layer on basin margins. Hueneme channel is considerably narrower than during the lowstand as a result of deposition of the inner levees. If this style of sedimentation is representative of marine highstands, then previous highstands may be represented by the intervals immediately below F and around B (Fig. 8). The lower of these intervals best exhibits these features and thus likely corresponds to the prolonged highstand of isotopic Stage 5 (Fig. 13). Such an interpretation is consistent with sedimentation rates in Santa Barbara Basin determined at ODP Site 893 (Fig. 8; Shorebased Scientific Party, 1994). Only short streams drain the coast ranges into Santa Barbara Basin, so that a lower overall sediment accumulation rate is expected compared with Santa Monica Basin, which was fed directly by the Ventura and Santa Clara rivers during lowstands (Dahlen *et al.*, 1990; Shorebased Scientific Party, 1994). This interpretation has subsequently been supported by preliminary results from ODP Site 1015, which indicate that the bottom of the hole, immediately above reflector C in our stratigraphic correlation, is younger than 60 ka (Shipboard Scientific Party, 1997).

Alternative chronologies cannot be excluded, but appear less probable. For example, the pronounced glacial period of isotopic Stage 6 (Illinoian glacial lowstand) might be interpreted as corresponding to the C to D interval, when there was a wide channel and high levee development on Hueneme fan and acoustically stratified sediment on the basin margin. Extrapolation of Nardin's (1981, 1983) Holocene sedimentation rate would be consistent with such an interpretation. This interpretation would place the long Stage 5 highstand above reflector D. Although there was considerable onlap of Dume fan in this interval (Fig. 6), the sediment accumulation on Hueneme fan was greater than on the basin floor. Furthermore, this would imply a substantially lower sedimentation rate on Hueneme fan, let alone in Santa Monica Basin, than in Santa Barbara Basin. It seems more likely that the event represented by the C to D interval corresponds to the isotopic Stage 4 lowstand (Fig. 13).

Growth patterns

The contrasting growth patterns of Hueneme and Dume fans reflects, in part, the shifting line source for Hueneme fan compared with the fixed point source, Dume Canyon, for Dume fan. For Dume fan, minor tectonic movement will have

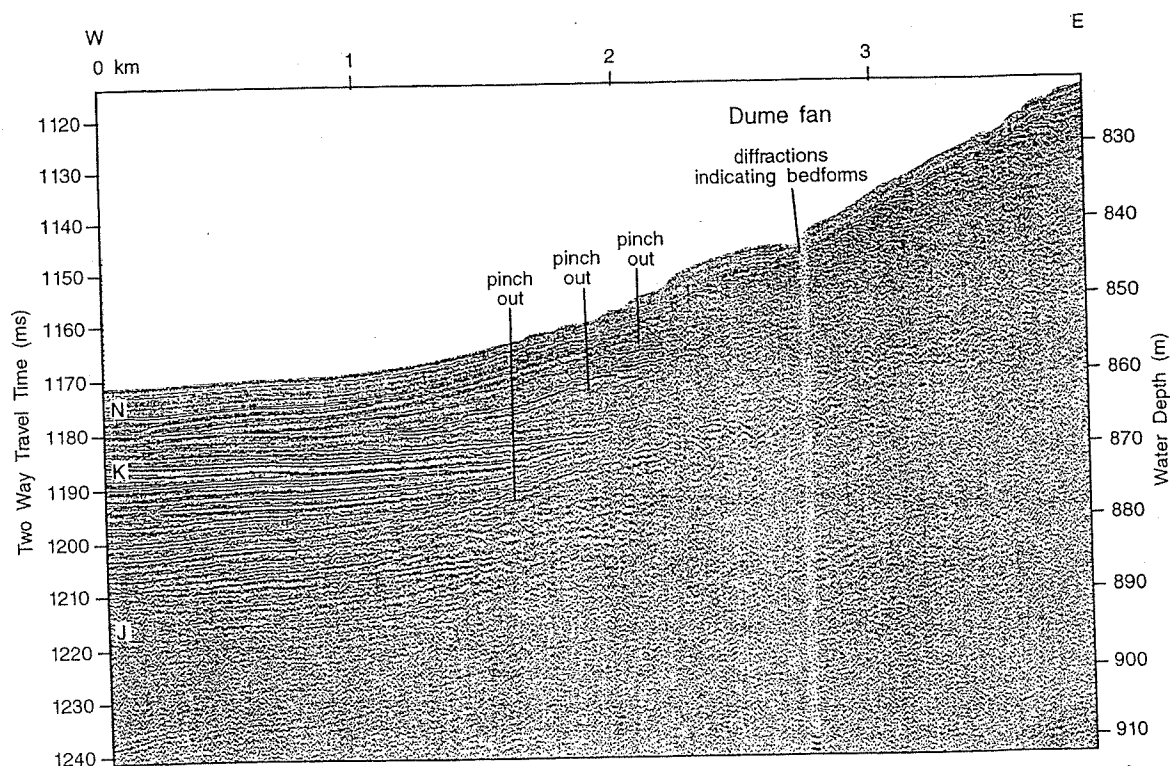


Fig. 11. Digitally processed deep-towed boomer record from line 54 showing near-surface facies developed on Dume fan. Interpreted line drawing of corresponding NSRF profile and location shown in Fig. 6.

effects indistinguishable from other causes of relative sea-level change. On Hueneme fan, tectonic tilting (Dahlen *et al.*, 1990) has the potential to cause shifts in sediment pathways that might mask some effects of eustatic sea-level change.

The late Quaternary Santa Monica Basin-fill is dominated by supply through the various pathways on Hueneme fan. During the last lowstand of sea level, rapid growth of the western levee of Hueneme Channel took place between reflectors J and N; levee growth west of channels (C) and (D) took place between reflectors G and J (Figs 5 and 8). These highly asymmetric levee systems imply deposition from thick turbidity currents influenced by the Coriolis force. The presence of mud waves, best developed on the levees of the Hueneme Channel system (Fig. 2), implies that the flows were also thick. Piper and Savoye (1993) have argued that such highly asymmetric valleys are built by slow flows of long duration and indicate hyperpycnal flow from rivers. Steep, small-to-medium-sized rivers such as the Santa Clara have been shown to be important sources of hyperpycnal flows (Mulder & Syvitski, 1995).

We interpret the general style of deposition between reflectors D and K on Hueneme fan as reflecting direct lowstand sediment input from the relatively sandy delta of the Santa Clara River

(Figs 13 and 14). Several distributaries were active, although likely not all simultaneously, and between reflectors G and K there was a progressive westward shift of the dominant distributary (line 36, Figs 3 and 5). Depositional thicknesses were greater on Hueneme fan than in Santa Monica Basin (Fig. 8). Extensive lenticular sheet sands were deposited on the middle fan, with greatest thicknesses downslope from the active distributary (e.g. line 42, Fig. 5).

In contrast, deposition above reflector K took place under rising or stable high sea-level conditions. Sedimentation on Hueneme fan largely draped pre-existing topography and Hueneme upper-fan valley was reduced to about 1 km wide, compared with 2–3 km wide between reflectors F and K (Figs 3b, 5a). This change in fan-valley width presumably reflects in some manner a change in the mean and/or maximum size of turbidity currents flowing through the system (see below). Sediment thickness is greater in Santa Monica Basin than on Hueneme fan (Figs 5, 8) resulting in ponding in the basin and onlap onto the lower fan. On Dume fan, there are at least three pinch-outs of coarse sediment (Fig. 11) in the time span represented by the last glacial maximum. This suggests considerable change in the fan-valley pattern over this time

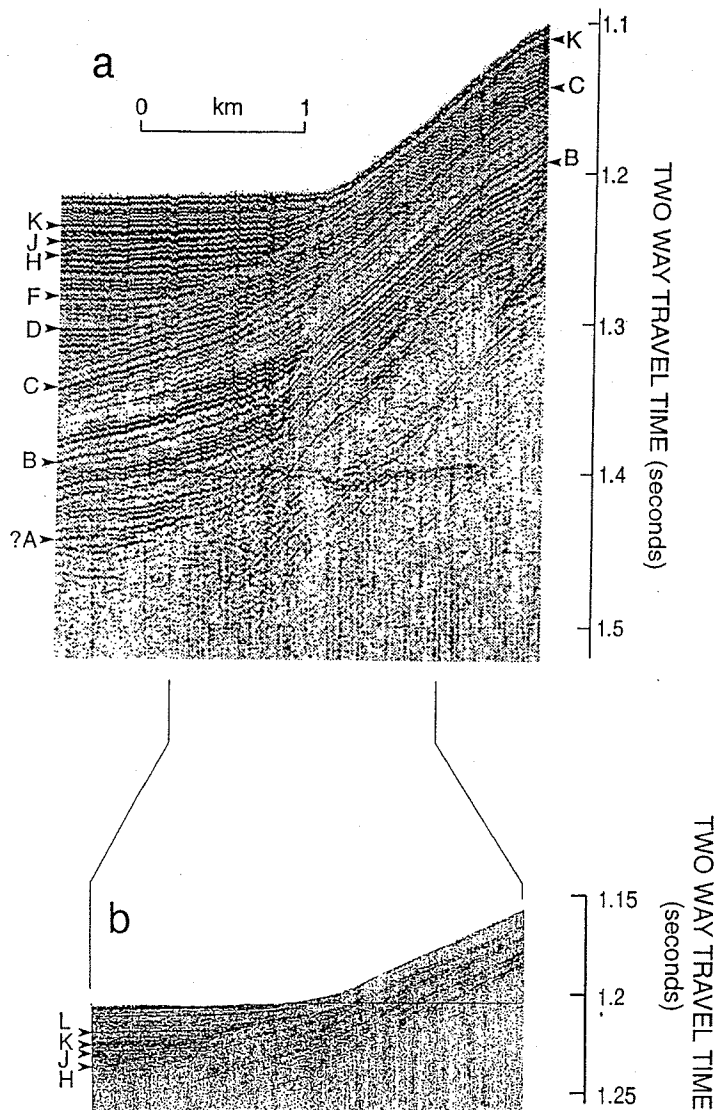


Fig. 12. Seismic-reflection profiles at southeastern margin of Santa Monica Basin showing relationship of amplitude of reflections to stratigraphic position. (a) sleeve gun with NSRF eel; (b) deep-towed boomer. Location shown in Fig. 1.

period – much more rapid change than on Hueneme fan. Because no river enters the sea at Dume Point (Fig. 1), Dume fan appears to have been fed by longshore drift at both high- and lowstands of sea level.

Highstand versus lowstand sedimentation

Although sea-level fluctuations do not change the basic processes of sediment transfer from the coastal zone to the basins, rapid sea-level rise may lead to partial filling of canyons that receive only a limited sediment supply (such as the Holocene Santa Monica Canyon: Nardin *et al.*, 1981). At sea-level lowstands, there is virtually no continental shelf (Fig. 14), and smaller shelf-edge gullies and canyons may become re-activated, so that river-derived mud is more likely to be

deposited directly in the basin opposite the river mouth.

The inferred contrast between highstand and lowstand conditions on Hueneme fan must be related in some manner to turbidity-current source and initiation processes (Fig. 14). Without more core data, we cannot develop a precise budget for sand and mud in the system. At lowstands, thick levees indicate significant mud deposition from turbidity currents; during the highstand, levees are proportionally thinner but the basin plain may receive less sand. Overall, it is not clear whether highstands or lowstands had a higher sand to mud ratio.

Analogy with modern sandy bedload deltas suggests that during sea-level lowstands, initiation of turbidity currents likely resulted either from sediment failure during rapid delta

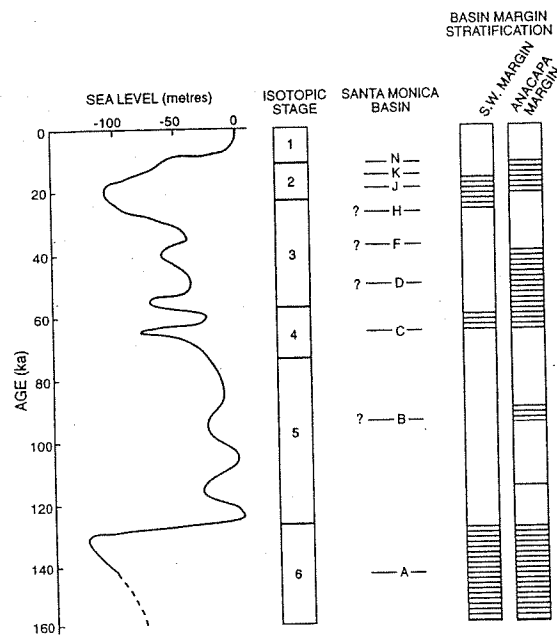
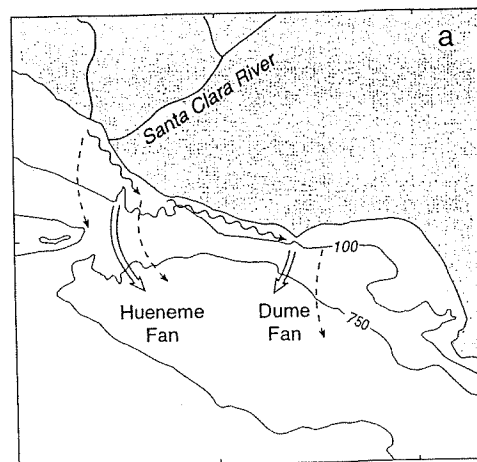


Fig. 13. Summary figure illustrating inferred chronology of the evolution of Hueneme fan in relation to sea-level change, key reflections in Santa Monica Basin, and amplitude of reflections on the basin margin. Sea-level curve from Flood and Piper (1995).

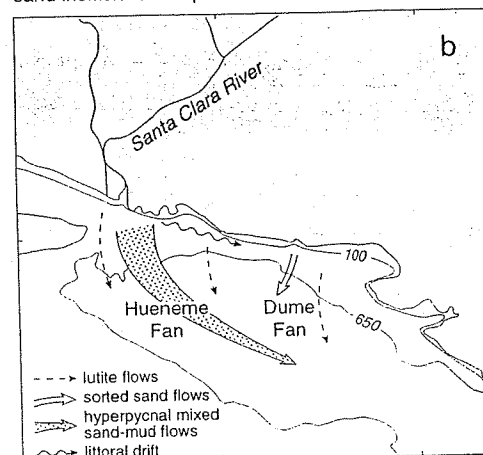
progradation or from hyperpycnal flow during floods (Fig. 14b). In either case, most sand-transporting flows would have contained a significant mud load with sand, allowing them to maintain their density contrast with seawater even after deposition of part of the sand load. Such flows are relatively efficient in carrying sand well out into a deep-water basin (Mutti, 1979). In the case of Hueneme fan, interpreted lowstand deposits beneath the modern middle fan (Fig. 5, line 42, between reflections D and N) are particularly sandy, consisting of sand lenses and sheets.

Those lowstand turbidity currents that were initiated by hyperpycnal flow were likely rich in mud, of long duration (perhaps days), and may have been quite thick (Normark & Piper, 1991). We believe that this type of flow is responsible for rapid progradation and maintenance of high levees with superimposed mud waves on Hueneme fan from reflector G time to reflector N time (Fig. 5, line 36). Similar growth of high mud-rich levees characterized the Var fan during lowstands of sea level (Piper & Savoye, 1993).

In contrast, the shallowest sediment on the fan, deposited under highstand conditions, is acoustically relatively transparent above reflector O (Fig. 3d). Extrapolation of ^{210}Pb accumulation rates (Christensen *et al.*, 1994) suggests that this unit accumulated in the last few thousand years. Gorsline (1996) suggested, based on box cores



HIGHSTAND
sandy flows from canyon heads
sand-inefficient transport



LOWSTAND
mixed sand-mud hyperpycnal flows
sand efficient transport

Fig. 14. Summary of sediment pathways and processes in Santa Monica Basin at (a) highstands and (b) lowstands.

from the youngest part of this unit, that in the last 500 years, turbidite deposits in Santa Monica Basin were related to major earthquakes and to exceptional river floods. The sediment below reflector O, likely accumulated during rising sea level, may have been deposited from turbidity currents generated from break-up of earthquake-triggered muddy slumps (Gorsline, 1996), or from a process similar to that determined for La Jolla Canyon, 150 km to the south, with large storms initiating rip-currents in canyon heads that re-suspend both sand and lesser mud (Inman *et al.*, 1976; Shepard *et al.*, 1977).

On Dume fan, canyon-fed flows were likely the only suppliers of sediment throughout sea-level cycles, with reduction in sediment supply during rising sea level (above N in Fig. 11). The sand

contributed to canyon heads by littoral cells would be quite well sorted, and the resulting turbidity currents would therefore be relatively inefficient in transporting the sand over long distances down the fan surface (Stacey & Bowen, 1988; Normark & Piper, 1991). This is because as sand, which is a major part of the suspended load before reaching the lower gradient fan, is deposited, there is insufficient mud remaining in suspension to continue to drive the flow. Only in cases where significant mud has advected off the shelf and accumulated in the canyon can an efficient flow develop. On Dume fan, inefficient sand transport is indicated by a rapid transition from inferred sand-rich to sand-poor facies at the break in slope at the toe of the fan (Figs 6 and 11).

An important characteristic of modern highstand sediment dispersal is that the mud load of coastal rivers is either sequestered in estuaries, is regionally dispersed in surface plumes extending seaward of the deltas (Emery & Milliman, 1978; Thornton, 1981, 1984), or is transported in lutite flows that cascade down basin slopes from the narrow shelf following storms (cf. Cacchione & Southard, 1974; McGrail & Carnes, 1983). These processes, combined with the action of littoral cells on the shelf, effectively segregate sand and mud components of the river contribution to the basin (Fig. 14a). The mud from surface plumes and lutite flows forms a blanket throughout the borderland basins that might account for the enhanced thickness of basin-floor deposits relative to fan deposits during the inferred highstand between reflector A time and reflector C time (Figs 8 and 13). In Santa Barbara Basin, grey mud layers derived from lutite flows are most common during periods of relatively high sea level although this may in part relate to better preservation due to non-bioturbation (Behl, 1995).

We suspect that the inferred change in turbidity-current characteristics that accompanied the Holocene sea-level rise is responsible for the striking change in width of the active part of the Hueneme fan valley from about 2–3 km to 1 km (Fig. 3b). The more subdued inner levees in the fan valley appear as marginal terraces within the older high levees. The lower, eastern inner levee contains 30–50% acoustically incoherent lenses in boomer profiles (Piper *et al.*, 1994), while the higher western inner levee consists of more typical levee facies similar to the adjacent high levee of Hueneme fan valley (Fig. 3c). The acoustically incoherent lenses are interpreted as sand turbidites. The general interbedding of these inferred thick sand beds with acoustically well-

stratified sediments is strikingly like the facies association seen in boomer profiles in the middle-fan sand sheets (Piper *et al.*, 1994). One hypothesis is that during sea-level rise, the inner-fan valley became partly backfilled with facies that had previously characterized middle-fan lobes (i.e., a landward shift of facies). Like streams and rivers that are described by geomorphologists as 'underfit' following a sharp reduction in annual discharge, the new equilibrium valley cross-section in Hueneme fan valley was significantly reduced by the backfilling process to match presumed smaller flow volumes, and the youngest valley is 'underfit' within higher levees that formed when sea level was low.

Aggradation versus progradation during fan growth

Models that have been developed to predict cyclicity and grain-size trends in submarine-fan deposits rest strongly on assumptions as to whether fan elements prograde or aggrade through time (Mutti & Ricci Lucchi, 1972; Hiscott, 1981; Ghibaudo, 1981). We define *progradation* as a shift in the area of more rapid sediment accumulation down a basin flank, so that the basin margin and the centroid of thicker deposition advances toward the basin centre; *aggradation*, conversely, implies more uniform vertical sediment accumulation across several sedimentary environments that can include the basin flank. Even in an aggradational setting, there may be basinward and landward *facies shifts* through time, but these do not constitute progradation in a morphological sense unless there is substantial asymmetric deposition promoted by the facies shift. The definition of progradation provided here is somewhat different from the definition of Normark *et al.* (1993), which recognizes progradation whenever facies boundaries shift basinward, even if the amount of vertical sediment accumulation is the same everywhere, leaving sea-floor morphology unaffected.

On Hueneme fan, the positions of major feeder valleys and the basinward limit of the fan do not appear to have changed significantly in the past 150 ka (Figs 5 and 9). In addition, the thickness of sediment deposited above reflector A is essentially invariant over the basin area (Figs 4 and 8). These observations both suggest that the growth of Hueneme fan has been characterized by long-term aggradation, not progradation. The only parts of Hueneme fan that have periodically prograded basinward are the high levees that

were active at times of low or falling sea level (e.g., Fig. 10, J-surface). This type of levee progradation is also common on much larger submarine fans (Flood & Piper, 1995; Flood *et al.*, 1995). Because of changes in sediment supply and the efficiency of sand transport by turbidity currents, fan facies have periodically shifted landward or basinward (Fig. 9).

In contrast, the smaller, sandier, canyon-fed Dume fan shows evidence for repeated progradation (Fig. 11), during which the tips of thicker sand wedges extended 1–2 km farther toward the basin centre than during times of reduced sand supply. Even in this case, however, the progradation is represented as short-lived growth stages near the toe of the fan, and the rapid aggradation of the basin-floor succession has prevented the fan from extending very far into the basin (Figs 6 and 11).

Application to seismic-stratigraphic interpretation and hydrocarbon exploration

The most important factors controlling sand-bed geometry on Hueneme fan and Santa Monica Basin are the source and textural composition of turbidity currents. Their character largely results from the interaction of relative sea-level position with the geomorphic framework of the continental shelf and shelf break. In this tectonically active environment, major changes in sedimentation can be related to eustatic sea-level history. Detailed history of individual valleys feeding Hueneme fan cannot be determined because of uncertainties about the amount and timing of tectonic tilting along the basin margin.

Efficient turbidity currents with a mixed sediment load, derived directly from deltaic input *via* sediment failure or hyperpycnal river discharge, deposit prominent sandy lobes on the middle fan that are 8–12 km wide and a few tens of metres thick. Lobe reflections downlap onto old fan surfaces (Fig. 7). In Santa Monica Basin, shifting of lobes is not simply an autocyclic process (compensation cycles of Mutti & Sonnino, 1981), but rather the result of shifts in sediment input to the upper fan (i.e., shifting input through Hueneme Canyon and valleys (C) and (D)), likely as a result of changes in the position of sandy delta distributaries. The upper-fan channels associated with these multiple input points appear highly stable as a result of the growth of high-relief western levees along active channels. These channels have been persistently re-occupied.

although the size of the talweg channel has varied through time.

At high stands of sea level, the lack of direct river supply of sediment to the shelf edge upslope from Hueneme fan restricts the possibility for generating turbidity currents that transport large amounts of sand efficiently. When the sediment load of sandy turbidity currents is particularly well sorted, as is the case when sand is trapped by shelf-edge canyons without significant advection of mud, turbidity currents are relatively inefficient in carrying the sand basinward, and sand is either confined to upper-fan channels or forms steep and small-radius bodies like Dume fan. Contemporary basin-floor sediments onlap older basin-margin fans, perhaps because mud is dispersed to the basin floor through sediment plumes and lutite flows, thickening the basin-floor succession.

CONCLUSIONS

- 1 Mixed sand-mud deposits of Hueneme fan consist of sandy channel facies and muddy high-levée facies of the upper fan, sandy sheet facies of the middle fan, and thinly bedded turbidite and hemipelagic facies on the lower fan, basin plain, and basin slopes.
- 2 Fifteen widely traceable seismic reflections and their inferred ages provide a framework for the interpretation of fan growth and development since about 160 ka.
- 3 At times of low sea level (oxygen isotopic Stages 2–4), poorly sorted, efficient turbidity currents were generated on the Santa Clara prodelta and sand was widely distributed in fan valleys and as lenticular sheets on the middle fan. Thick mud-load turbidity currents, presumed to originate in hyperpycnal river flows, promoted the rapid downfan progradation of high right-hand levees along valleys on the upper fan. A line source of 3–4 upper-fan valleys and their associated levees were active at different times during the last sea-level lowstand, presumably because of switches in the positions of delta distributaries at the coast. Fan deposits are somewhat thicker than basin-floor deposits at times of low sea level.
- 4 At times of high sea level (above –30 m during oxygen isotopic Stages 5 and 1), there is more segregation of delivery of mud and sand to basin. Some mud takes independent routes to the fan and basin *via* advection in surface plumes and storm-generated lutite flows. Basin-floor deposits are locally thicker than contemporary fan deposits. Upper fan channels become partly backfilled

by sand and mud forming inner levees that confine flows to underfit talweg channels. Sediment supply to steep sandy fans (e.g., Dume fan) is reduced.

5 Despite the active margin tectonics, major sedimentation changes can be related to eustatic sea-level changes.

ACKNOWLEDGMENTS

We thank the officers, crew, and technical staff of the Geological Survey of Canada (GSC), who participated on *CSS Parizeau* cruise 91-062, for their invaluable assistance in gathering seismic data. Mr Roy Sparkes (GSC) was particularly helpful in preparation of trackplots and bathymetric map. Mr Martin Guerrero Suastegui, Universidad Autonoma de Guerrero, assisted in data collection at sea. The paper was improved by reviews by Rick Behl, Kim Klitgord and Ken Skene. Participation of RNH in this project is supported through grants from the Natural Sciences and Engineering Research Council of Canada. This is Geological Survey of Canada contribution number 1996-503

REFERENCES

- Behl, R.J. (1995) Sedimentary facies and sedimentology of the late Quaternary Santa Barbara Basin, Site 893. *Proc. ODP, Sci. Results*, **146 (Pt 2)**, 295-305.
- Cacchione, D.A. and Southard, J.B. (1974) Incipient sediment movement by shoaling internal gravity waves. *J. Geophys. Res.*, **70**, 2237-2242.
- Christensen, C.J., Gorsline, D.S., Hammond, D.W. and Lund, S.P. (1994) Non-annual laminations and expansion of anoxic basin floor conditions in Santa Monica Basin, California Borderland, over the past four centuries. *Mar. Geol.*, **116**, 399-418.
- Crouch, J.K. and Suppe, J. (1993) Late Cenozoic tectonic evolution of the Los Angeles basin and inner California borderland: A model for core complex-like crustal extension. *Bull. Geol. Soc. Am.*, **105**, 1415-1434.
- Dahlen, M.Z., Osborne, R.H. and Gorsline, D.S. (1990) Late Quaternary history of the Ventura mainland shelf, California. *Mar. Geol.*, **94**, 317-340.
- Edwards, B.D., Field, M.E. and Kenyon, N.H. (1996) Morphology of small submarine fans, inner California Continental Borderland. In: *Geology of the United States' Seafloor: The View from GLORIA* (Ed. by J.V. Gardner, M.E. Field and D.G. Twitchell), Cambridge University Press, Cambridge. pp. 235-249.
- EEZ-SCAN 84 Scientific Staff (1986) *Atlas of the Exclusive Economic Zone, Western Conterminous United States*. U.S. Geol. Survey Misc. Invest. Series I-1792, scale 1:500 000, 152 pp.
- Emery, K.O. and Bray, E.E. (1962) Radiocarbon dating of California basin sediments. *Bull. Am. Assoc. Petrol. Geol.*, **46**, 1839-1856.
- Emery, K.O. and Milliman, J.D. (1978) Suspended matter in surface waters: influence of river discharge and of upwelling. *Sedimentology*, **25**, 125-140.
- Flood, R.D. and Piper, D.J.W. (1995) Introduction. In: *Initial Reports of the Ocean Drilling Program, Vol. 155* (Ed. by R.D. Flood, D.J.W. Piper and A. Klaus), pp. 5-13. Ocean Drilling Program, College Station.
- Flood, R.D., Piper, D.J.W., Klaus, A. et al. (1995) *Initial Reports of the Ocean Drilling Program, Vol. 155*. 1233 p. Ocean Drilling Program, College Station.
- Ghibaudo, G. (1981) Deep-sea fan deposits in the Macigno Formation (middle-upper Oligocene) of the Gordana Valley, northern Apennines, Italy — reply. *J. Sedim. Petrol.*, **51**, 1021-1033.
- Gorsline, D.S. (1996) Depositional events in Santa Monica Basin, California Borderland, over the past five centuries. *Sedim. Geol.*, **104**, 73-88.
- Gorsline, D.S. and Emery, K.O. (1959) Turbidity-current deposits in San Pedro and Santa Monica basins off southern California. *Bull. Geol. Soc. Am.*, **70**, 279-290.
- Heusser, L.E. (1995) Pollen stratigraphy and paleoecologic interpretation of the 160-k.y. record from Santa Barbara Basin, Hole 893A. *Proc. ODP, Sci. Results*, **146 (Pt 2)**, 265-280.
- Hiscott, R.N. (1981) Deep-sea fan deposits in the Macigno Formation (middle-upper Oligocene) of the Gordana Valley, northern Apennines, Italy — discussion. *J. Sedim. Petrol.*, **51**, 1015-1021.
- Inman, D.L., Nordstrom, C.E. and Flick, R.E. (1976) Currents in submarine canyons: an air-sea-land interaction. *Ann. Rev. Fluid Mech.*, **8**, 275-310.
- Kennett, J.P. (1995) Latest Quaternary benthic oxygen and carbon isotope stratigraphy: Hole 893A, Santa Barbara Basin, California. *Proc. ODP, Sci. Results*, **146 (Pt 2)**, 3-18.
- Klitgord, K.D. and Brocher, T.M. (1996) Oblique-slip deformation in the San Pedro basin offshore southern California. *Eos, Trans. AGU*, **77**, F737.
- Malouta, D.N., Gorsline, D.S. and Thornton, S.E. (1981) Processes and rates of filling of an active transform margin: Santa Monica Basin, California continental borderland. *J. Sedim. Petrol.*, **51**, 1077-1095.
- McGrail, D.W. and Carnes, M. (1983) Shelfedge dynamics and the nepheloid layer in the northwestern Gulf of Mexico. In: *The Shelfbreak: Critical Interface on Continental Margins* (Ed. by D.J. Stanley and G.T. Moore), *Spec. Publ. Soc. Econ. Paleontol. Mineral.*, **33**, 251-264.
- Milliman, J.C. and Syvitski, J.P.M. (1992) Geomorphic/tectonic control of sediment discharge to the ocean: the importance of small mountainous rivers. *J. Geol.*, **100**, 525-544.
- Mulder, T. and Syvitski, J.P.M. (1995) Turbidity currents generated at mouths of rivers during exceptional discharges to the world oceans. *J. Geol.*, **103**, 285-299.

- Mutti, E. (1979) Turbidites et cônes sous-marins profonds. In: *Sédimentation Détritique (fluviale, littorale et marine)* (Ed. by P. Homewood). pp. 353–419. Institut Géologique d'Université de Fribourg.
- Mutti, E. (1985) Turbidite systems and their relations to depositional sequences. In: *Provenance of Arenites* (Ed. by G.G. Zuffa), pp. 65–93. Reidel, Dordrecht.
- Mutti, E. (1992) *Turbidite Sandstones*. Agip and Università di Parma, Parma.
- Mutti, E. and Ricci Lucchi, F. (1972) Le torbiditi dell'Apennino settentrionale: introduzione all'analisi di facies. *Mem. Soc. Geol. Italy*, **11**, 161–199.
- Mutti, E. and Sonnino, M. (1981) Compensation cycles: a diagnostic feature of sandstone lobes. In: *Abstracts, European Regional Meeting (Bologna, Italy), Int. Assoc. Sedimentol.* (Ed. by R. Valloni, A. Colella, M. Sonnino, E. Mutti, G.G. Zuffa and G.G. Ori). pp. 120–123.
- Nardin, T.R. (1981) *Seismic stratigraphy of Santa Monica and San Pedro Basins, California continental borderland: late Neogene history of sedimentation and tectonics*. Ph. D. thesis, University of Southern California, Los Angeles.
- Nardin, T.R. (1983) Late Quaternary depositional systems and sea level changes—Santa Monica and San Pedro Basins, California Continental Borderland. *Bull. Am. Assoc. Petrol. Geol.* **67**, 1104–1124.
- Nardin, T.R., Osborne, R.H., Bottjer, D.J. and Schneidermann, R.C. (1981) Holocene sea level curve for Santa Monica Shelf, California continental borderland. *Science*, **213**, 331–333.
- Normark, W.R. and Piper, D.J.W. (1991) Initiation processes and flow evolution of turbidity currents: implications for the depositional record. In: *From Shoreline to Abyss: Contributions in Marine Geology in Honor of Francis Parker Shepard* (Ed. by R.H. Osborne), *Spec. Publ. Soc. Econ. Paleontol. Mineral.*, **46**, 207–230.
- Normark, W.R., Piper, D.J.W. and Hess, G.R. (1979) Distributary channels, sand lobes, and mesotopography of Navy submarine fan, California borderland, with applications to ancient fan sediments. *Sedimentology*, **26**, 749–774.
- Normark, W.R., Posamentier, H. and Mutti, E. (1993) Turbidite systems: state of the art and future directions. *Rev. Geophys.*, **31**, 91–116.
- Piper, D.J.W. and Savoye, B. (1993) Processes of late Quaternary turbidity current flow and deposition on the Var deep-sea fan, north-west Mediterranean Sea. *Sedimentology*, **40**, 557–582.
- Piper, D.J.W., Normark, W.R. and Hiscott, R.N. (1994) 28. Holocene sand-body geometry, Hueneme Fan, California Borderland. In: *Atlas of Deep Water Environments* (Ed. by K.T. Pickering, F. Ricci Lucchi, R.D.A. Smith, N.H. Kenyon and R.N. Hiscott), pp. 203–206. Chapman and Hall, Andover, Hants.
- Posamentier, H.W., Jervey, M.T. and Vail, P.R. (1988) Eustatic controls on clastic deposition. I. In: *Sea Level Change — an Integrated Approach* (Ed. by C.K. Wilgus, B.S. Hastings, C.G. St. C. Kendall, H.W. Posamentier, C.A. Ross and J.C. Van Wagoner), *Spec. Publ. Soc. Econ. Paleontol. Mineral.* **42**, 109–124.
- Reynolds, S. (1987) A recent turbidity current event, Hueneme fan, California: reconstruction of flow properties. *Sedimentology*, **34**, 129–137.
- Schwalbach, J.R. and Gorsline, D.S. (1985) Holocene sediment budgets for the basins of the California continental borderland. *J. Sedim. Petrol.*, **55**, 829–842.
- Shepard, F.P., McLoughlin, P.A., Marshall, N.F. and Sullivan, G.G. (1977) Current-meter recording of low speed turbidity currents. *Geology*, **5**, 297–301.
- Shipboard Scientific Party (1997) Site 1015. In: *Proc. ODP, Init Repts.*, **167**: College Station, Texas (Ocean Drilling Program) (in press).
- Shorebased Scientific Party (1994) Site 893. In: *Initial Reports of the Ocean Drilling Program*, Vol. 146, pt. 2, (Ed. by J.P. Kennett, J. Baldauf et al.), Ocean Drilling Program, College Station, 15–50.
- Stacey, M. W. and Bowen, A. J. (1988) The vertical structure of turbidity currents and a necessary condition for self-maintenance. *J. geophys. Res.*, **93**, 3543–3553.
- Teng, L.S. and Gorsline, D.S. (1989) Late Cenozoic sedimentation in California Continental Borderland basins as revealed by seismic facies analysis. *Bull. Geol. Soc. Am.*, **101**, 27–41.
- Thornton, S.E. (1981) Suspended sediment transport in surface waters of the California Current off southern California: 1977–78 floods. *Geo-Marine Letts.* **1**, 23–28.
- Thornton, S.E. (1984) Basin model for hemipelagic sedimentation in a tectonically active continental margin: Santa Barbara Basin, California Continental Borderland. In: *Fine-grained sediments: deep water processes and facies* (Ed. by D.A.V. Stow and D.J.W. Piper), *Geol. Soc. Lond. Spec. Publ.*, **15**, 377–394.
- Vedder, J.G. (1987) Regional geology and petroleum potential of the Southern California Borderland. In: *Geology and resource potential of the continental margin of western North America and adjacent ocean basins — Beaufort Sea to Baja California* (Ed. by D.W. Scholl, A. Grantz and J.G. Vedder), *Circum-Pacific Council for Energy and Mineral Resources, Ear. Sci. Ser.*, **6**, 403–447.

Manuscript received 17 April 1996; revision accepted 27 March 1997.

anisotropy is difficult to constrain, so the data are compared to synthetics to narrow the possible models responsible for the splitting. Differential travel times between S(Sdiff)(SH)-SKS(SV) and ScS(SH)-S(SH) are used to deduce isotropic heterogeneity in D", with the times corrected for aspherical mantle structure above D". We calculate differential travel time residuals with respect to PREM averaging 0.04 s for S-SKS and 0.25 s for ScS-S. Heterogeneity inferred from S-SKS differential times was averaged to be 0.62% and for and ScS-S was 1.2% which agrees well with high-resolution tomographic model predictions. All data are inspected for Scd arrivals, the seismic phase attributed to a reflection off a high velocity layer in D", to assess the possible presence of a D" discontinuity. In contrast to high velocity regions of the circum-Pacific and the low velocity central Pacific, our results show relatively reduced magnitudes of anisotropy in a region characterized as a transition from high-to-low isotropic heterogeneity (west-to-east). We relate these patterns to deep mantle dynamics and discuss implications of our observations for boundary layer processes.

S12E MCC: 105 Monday 1630h

Gutenberg Lecture (joint with DI)

Presiding: J E Vidale, University of California, Los Angeles Inst. Geophys. Planet. Phys.

S12E-01 1640h INVITED

Bananas, Doughnuts and Seismic Traveltimes

Francis A Dahlen (1-609-258-4130; fad@princeton.edu)

Department of Geosciences, Princeton University, Princeton, NJ 08544, United States

Most of what we know about the 3-D seismic heterogeneity of the mantle is based upon ray-theoretical traveltime tomography. In this infinite-frequency approximation, a measured traveltime anomaly depends only upon the wavespeed along an infinitesimally thin geometrical ray between a seismic source and a seismic station. In this lecture I shall describe a new formulation of the seismic traveltime inverse problem which accounts for the ability of a finite-frequency wave to "feel" 3-D structure off of the source-receiver ray. Finite-frequency diffraction effects associated with this off-ray sensitivity act to "heal" the corrugations that develop in a wavefront propagating through a heterogeneous medium. Ray-theoretical tomography is based upon the premise that a seismic wave "remembers" all of the traveltime advances or delays that it accrues along its path, whereas actual finite-frequency waves "forget". I shall describe a number of recent analytical and numerical investigations, which have led to an improved theoretical understanding of this phenomenon.

S21A MCC: Hall C Tuesday 0830h

Seismicity and Stress on the San Andreas Fault System Posters (joint with G, T, MR)

Presiding: C M Rubin, Central Washington University; **E Roeloffs**, U.S. Geological Survey

S21A-0965 0830h POSTER

Examining Structural Controls on Earthquake Rupture Dynamics Along the San Andreas Fault

Jeffrey J McGuire¹ (508-289-3290; jmcguire@whoi.edu)

Yehuda Ben-Zion² (1-213-740-6734; benzion@terra.usc.edu)

¹ Woods Hole Oceanographic Institution, Dept of Geology and Geophysics, MS24, Woods Hole, MA 02543, United States

² University of Southern California, Department of Earth Sciences, Los Angeles, CA 90089-0740, United States

Recent numerical simulations of dynamic rupture [Andrews and Ben-Zion, 1997; Harris and Day, 1997] have confirmed earlier analytical results [Wuertman, 1980; Adams, 1995] that a contrast in elastic properties

between the two sides of a fault will generate an interaction between the normal stress and fault slip that is not present in a homogeneous medium. It has been shown that for a range of frictional parameters and initial conditions, this interaction produces a statistical preference for unilateral rupture propagation in the direction of slip of the more compliant medium [Ben-Zion and Andrews, 1998; Cochard and Rice, 2000; Ben-Zion and Huang 2002]. Thus, the directivity of earthquake ruptures on large faults with well-developed material interfaces may be controlled by material contrasts of the rocks within and across the fault zone.

One of the largest known velocity contrasts across a major crustal fault occurs along the Bear Valley section of the San Andreas where high velocity materials on the SW side (P-velocity >5 km/s) are juxtaposed with low-velocity material on the NE side (P-velocity <4 km/s) down to a depth of about 4 km with a less dramatic contrast continuing to about 8 km [Thurber et al., 1997]. This boundary is strong enough to generate significant head-waves refracted along it that are recorded as the first arrivals at stations close to the fault on the NE side [McNally and McEvilly, 1977; Rubin and Gillard [2000] and Rubin [2002] relocated the events in this region using NCSN waveform data and found that more than twice as many immediate aftershocks to small earthquakes occurred to the NW of the mainshock as to the SE, which they interpreted as being consistent with a preferred rupture direction to the SE. Their interpretation that aftershocks to microearthquakes occur preferentially in the direction opposite of rupture propagation has not been directly tested and is inconsistent with observations from moderate [Fletcher and Spudich, 1998] and large earthquakes [Kilb et al., 2000], which show considerable variability and possibly the opposite preference.

We are attempting to directly test the prediction of a preference for rupture propagation to the SE on this fault segment by combining travel-time and waveform modeling of fault-zone head waves, high precision earthquake relocations, and rupture directivity studies. Initial results indicate that there is considerable variability along strike in the strength of the across-fault velocity contrast, with maximum values reaching about 25-30%. This spatial variability in the strength of the material property contrast would be expected to produce a spatial variability in earthquake rupture directivity. We are developing a catalog of earthquake rupture directivity estimates for magnitude 2 and larger earthquakes to compare with the variations of the velocity contrast and aftershock asymmetry. Initial results indicate that even in the regions of highest velocity contrast, moderate earthquakes (M=3) can still rupture unilaterally to the NE. Detailed high resolution results from head-wave modeling, rupture directivity studies, and earthquake relocations will be presented.

S21A-0966 0830h POSTER

SCEC 3D Community Fault Model for Southern California

Andreas Plesch¹ (617-495-2356;

andreas.plesch@harvard.edu); John H Shaw¹ (shaw@eps.harvard.edu); James Dolan (dolan@earth.usc.edu); Lisa Grant (lgrant@uci.edu); Egill Hauksson (hauksson@gps.caltech.edu); Marc Kamberling (marc@quake.crustal.usc.edu); Mark Legg (mrllegg@atglobal.net); Scott Lindvall (lindvall@lettis.com); Craig Nicholson (craig@quake.crustal.usc.edu); Tom Rockwell (tom.rockwell@geology.sdsu.edu); Christopher Sorlien (chris@quake.crustal.usc.edu); Robert Yeats (yeats@mail.science.orst.edu)

¹ Harvard University, 20 Oxford St., Cambridge, MA 02144, United States

We present a new community-based, coarse-resolution 3D fault model (CFM-A 1.0) of southern California developed by the Southern California Earthquake Center (SCEC). The regional model extends from 32.5°N to 36°N, and from 114.5°W to 120.5°W. The object-oriented, CAD-based model provides three-dimensional representations of major strike-slip, blind-thrust, and oblique-reverse faults in a precise geographic reference frame. The fault geometries were established using published sources, surface traces, seismicity, seismic reflection profiles, well bore data, and other subsurface imaging techniques. Each fault is represented by a triangulated surface (ASCII format).

The model provides a list of "preferred" representations that are extracted from a relational database (Postgresql), which will be searchable by users via a web-interface based on Mapserver. The database contains a unique naming and numbering system for each fault (based on the CGS system), as well as various attributes including the fault type, slip rate (from CGS and SCFAD), uncertainties, quality of representation, and key references. Most faults have distinct interpolated and extrapolated segments, and many have alternative representations. Users will be able to access released versions of the model, or to create their own models via the web-interface and database. The model is intended for use in seismic hazards assessment, velocity modeling and fault systems analysis.

URL: <http://structure.harvard.edu/cfma>

along with systematic investigation of receiver effects. One possibility suggested by our preliminary analysis is that the discontinuity is strongly distorted, and possibly even shallower in the mantle than in the region to the north, causing the triplication to overlap with direct S. There is also some evidence for a region with two smaller shear velocity discontinuities. Characterized by the small scale lateral variations in D" structure this localized region provides a test of various interpretations of the D" discontinuity, including the possibilities of a phase change, a relic slab anomaly, a heterogeneous scattering layer, and a transition to an anisotropic structure in the thermal boundary layer. It is clear that dense station deployments are critical for resolving heterogeneous structure in D".

S12D-09 1550h

Lateral Variations of the D" Discontinuity Beneath the Central Pacific

Megan Avants¹ (831-459-3164; mavants@es.ucsc.edu)

Thorne Lay¹ (831-459-3164; tlay@es.ucsc.edu)

Earth Sciences Department, University of California Santa Cruz, Earth and Marine Sciences Bldg., Santa Cruz, CA 95064, United States

The lowermost 250 km of the mantle is characterized by a laterally heterogeneous thermal and chemical boundary layer, the D" Region. In many areas a strong velocity gradient or velocity discontinuity is found near the top of D", which is variously interpreted as being the result of a phase change, a chemical contrast, a transition in fabric to an anisotropic layer, a relic subducted slab thermal/chemical anomaly. Seismic waves from events in the Tonga-Fiji region enter the D" zone beneath the Central Pacific and are recorded by dense broadband seismic networks in western North America. Recent waveform stacking effects suggest the presence of coincident P and S velocity discontinuities about 230 km above the core-mantle boundary under the Central Pacific. The velocity contrasts at the discontinuities are weaker (0.75% and 1.7%, respectively) than found in circum-Pacific regions. It is also found that the S wave velocity decreases below the D" discontinuity is abnormally strong with respect to the P velocity decrease in this region, being far removed from present subduction zones. The existence of D" discontinuities in the low velocity mantle under the central Pacific is particularly intriguing. Lateral heterogeneities within this zone, combined with complex crustal structure at the receivers, make the depth and magnitude of the velocity discontinuities difficult to resolve. We extend analysis of shear wave data from the Tonga-Fiji region recorded by broadband networks in western North America to better resolve small scale features in D" under the Central Pacific. Our approach includes deconvolving reference source wavelets, binning and stacking localized subsets of data, and modeling features in the stacks to provide improved resolution of the nature of the D" discontinuity beneath the central Pacific. We compare these results to D" structure in circum-Pacific regions to gain insight as to the cause of D" discontinuities.

S12D-10 1605h

D" Anisotropy Beneath the Atlantic Ocean and the Southern Pacific Ocean

Elissa M Moore¹ (480-965-7680; emmoore@asu.edu)

Edward J Garnero¹ (480-965-7653; garnero@asu.edu)

Thorne Lay² (831-459-3164; tlay@es.ucsc.edu)

Arizona State University, Department of Geological Sciences Box 871404, Tempe, AZ 85287, United States

University of California Santa Cruz, Earth Sciences Department 1156 High Street, Santa Cruz, CA 95064, United States

Using data from South American earthquakes recorded by seismic stations in Europe and Africa, and Tonga-Fiji events recorded in South America with these paths from South America events to Tonga stations, we investigate properties of D" beneath the Atlantic and the southern Pacific. By measuring splits between the SV and SH components of ScS and S or split phases, we infer D" anisotropy magnitude. Broadband data, along with some digitized analog WWSSN data, were analyzed for deep focus earthquakes (> 100 km). All data are corrected for predictions of upper mantle anisotropy, and we assume that D" has vertically transverse isotropy (VTI) in our initial analysis. Beneath the Atlantic we find SV-SH splits averaging 2 s (minimum = -0.9 s; maximum = 3.6 s) in the northern regions where path coverage is densest and averaging 0.3 s (minimum = -1.6 s; maximum = 1.7 s) in the south Atlantic. Approximate strength of inferred anisotropy averages around 0.4% in the northern regions and 0.2% in the south. The geometry of

Council Ponders Negative LNG Report

18 January 2006 –

<http://www.pembrokeshiretv.com/content/templates/v6-article.asp?articleid=1270>

THE rose-tinted image of a 21st Century Pembrokeshire grown rich on the energy industry has been dealt a savage blow after it emerged that the largest single impact made by the county's two Liquefied Natural Gas terminals has been negative.

According to the document, entitled Social Impacts of LNG and due to be considered by the county council's economic committee tomorrow, the effect on the Pembrokeshire's housing market has led to spiralling costs in both the purchase and rental markets, massive increases in homelessness and a worsening of the already considerable difficulties faced by the county's young adults in trying to set up home.

While the report accepts that although the number migrant workers employed at the sites is less than originally predicted, the construction of the facilities has still seen landlords evicting long-term tenants to make way for higher-paying LNG workers.

The report describes how LNG workers are themselves buying up properties at inflated rates -further pushing home ownership beyond the reach of Pembrokeshire residents - and claims that the county now has the second highest house price to income ratio of anywhere in Wales.

The report also notes that during July to September last year, the number of homelessness applications received by the county council "increased substantially when a reduction in applications would have been expected".

The report's findings are based, in part, on interviews with five Milford Haven estate agents, all of whom agreed that "first time buyers have no chance".

The interviewees all said that the lower end of the housing market, homes valued at under £150,000, has witnessed a 20% price hike since construction of the LNG plants began. All those interviewed said they had first-hand experience of tenant evictions, with landlords often letting a room to two workers at a time, leading to single rooms reaping monthly incomes of up to £1000.

The report even claims that the lack of affordable housing caused by the LNG projects is having a detrimental effect on recruitment in the health service as medical staff, faced with the prospect of having nowhere to live in the county, were now being forced to seek employment elsewhere.

In addition to housing issues, The LNG facilities will, and indeed are, already having a significant impact on the county's transport infrastructure.

"There is a need for a strategic road network of sufficient capacity to service the Milford Haven Waterway which will be the UK's second largest port and largest concentration of energy supply," said the report.

To this end, the report concluded, a comprehensive review needed to be undertaken to investigate the possibility of by-passes for Milford Haven, Johnston, Haverfordwest and Pembroke.

Tomorrow's committee will also be asked to consider the additional burden the developments have placed on local policing.

The report states that between May and October last year, Dyfed Powys Police officers investigated approximately 30 criminal incidents involving LNG employees, ranging from rape to allegations of theft.

The sexual assault offence alone cost the force £9,000, including £5,000 interpreter costs, and 120-man hours to investigate.

The report goes to great length to emphasise the concerns of local people regarding the developments in terms of safety, housing and the perceived failure of the local authority to agree adequate compensation from the gas companies for affected communities.

The report states the need for "better communication of the 'National Interest' argument and the importance of these developments to the UK economy," as a means to mollify public opposition to the projects.

Social Impacts of LNG has not gone down well with local MP Stephen Crabb, who had previously backed the developments.

"I was very concerned to read the report," the Preseli Pembrokeshire MP said, "[..] It does raise some vitally important issues which cannot be ignored."

"Right from the start of the LNG projects I have said that there must be an economic and social pay-off for the people of Pembrokeshire. We have seen an increase in economic activity in the county and a continued fall in unemployment. However, there are unquestionably added pressures being placed on key local services, most importantly housing and transport."

Mr Crabb echoed much of the local feeling when he said the developers should be paying a higher price to construct the facilities in Pembrokeshire.

"Given the size and complexity of the projects, I think it is right that LNG developers foot the bill for the planning work carried out at County Hall. The Planning Department has been under huge pressure in recent years and LNG has contributed to that," he said.

He also criticised the initial agreements between the company and the county council to compensate local communities forced to live in the shadow of the facilities.

"I was disappointed that the original Section 106 Agreements were so thin; I still believe the Council could have got more without risking an appeal from the developers."

"The two LNG projects must leave a legacy for Pembrokeshire in terms of real improvements to the quality of life for local people. I want to see visible improvements in the communities of Waterston and Herbrandston and significant improvements in the road network serving the construction sites."

The Social Impact of LNG will be considered by the county council's Economic Overview and Scrutiny Committee from 10am tomorrow.

Pembrokeshire TV

<http://www.pembrokeshiretv.com/> This article has been brought to you by pembrokeshiretv.com. Please respect any copyrights for images and content.

PA Gov. Rendell Signs Measure Enacting Clean Energy Portfolio Standard in PA

CONSHOHOCKEN, Pa., Dec 16, 2004 /PRNewswire

Pennsylvania Governor Edward G. Rendell has signed into law a clean energy portfolio standard that will cut energy costs, promote economic development and encourage technologies to protect and restore the environment by ensuring more electricity generation comes from environmentally beneficial resources. Part of that effort includes \$10 million in new investments that the Governor authorized for clean power plants, enhancing Pennsylvania's reputation as a national energy leader.

"Cleaner, more advanced energy has its own rewards, in terms of both the environmental benefits it brings and the economic opportunities it promises," Governor Rendell said during a ceremonial bill signing at BJ's Wholesale Club, which has 1,400 solar panels on its warehouse roof. "By ensuring a diverse supply of clean and advanced energy, Pennsylvania is leading the way to address today's energy challenges and meet tomorrow's energy demands --- all while taking tremendous strides to make our environment healthier and cleaner."

The Governor signed into law a two-tiered portfolio standard that ensures in 15 years, 18 percent of all of the energy generated in Pennsylvania comes from clean, efficient sources. Act 213 of 2004 makes the Commonwealth the 18th state to adopt a renewable and advanced energy production provision.

Tier I requires 8 percent of electricity sold at retail in the state to come from traditional renewable sources such as solar photovoltaic energy, wind power, low-impact hydropower, geothermal energy, biologically derived methane gas, fuel cells, biomass energy or coal-mine methane. Notably, at least 0.5 percent of Tier I electricity must come from solar power -- a requirement that is at least three times more ambitious than anything any neighboring states have put in place and one that enhances the state's reputation as a clean energy leader.

Tier II requires 10 percent of the electricity to be generated from waste coal, distributed generation systems, demand-side management, large-scale hydropower, municipal solid waste, generation from pulping and wood manufacturing byproducts, and integrated combined coal gasification technology.

BJ's Wholesale Club was the largest solar generation facility in Pennsylvania in 1999. The company teamed up with Green Mountain Energy and Sun Power Electric to install 1,400 solar panels on the roof of its warehouse. The 60-kilowatt array will generate 65,526 kilowatt hours of clean electricity each year for 20 years for the club, which provides members with a variety of wholesale merchandise. Over its lifetime, this installation will prevent approximately 4,603 pounds of smog-producing nitrogen oxide; 14,760 pounds of sulfur dioxide, which creates acid rain; and 1.96 million pounds of carbon dioxide.

"The bill's renewable energy provisions will ensure that Pennsylvania is on the cutting edge of new energy technologies, making us more attractive to advanced energy companies seeking to take advantage of our location

2/28/2006

among other proliferation of portfolio standards," said Governor Rendell, who first unveiled a portfolio standard in his Feb. 3 budget address. "Likewise, the responsible use of resources such as waste coal will help to clean up mine-scarred landscapes while improving the quality of our streams and rivers by eliminating a source of acid mine drainage -- one of the most pressing environmental problems in our Commonwealth."

A recently published study by the global engineering firm Black and Veatch Corp. Inc. found significant economic benefits over and above pursuing business as usual with only traditional fuel sources. The benefits include \$10 billion in increased output for Pennsylvania, \$3 billion in additional earnings and between 3,500 and 4,000 new jobs for residents over the next 20 years. The study also indicates that for every 1 percent decrease in natural gas demand, there would be a corresponding \$140 million in savings to natural gas and electricity consumers.

The environmental benefits are significant, too. The clean energy portfolio standard as proposed would annually avoid 9,044,615 tons of carbon dioxide, 78,462 tons of sulfur dioxide, and 21,398 tons of nitrogen oxide. Pennsylvania surface water and rural communities will enjoy additional benefits from the continued remediation of waste coal deposits around the state, thus eliminating detrimental acid discharges to our waterways and restoring the land they occupied.

Governor Rendell already has mobilized appreciable new funds that can be put to work for energy in Pennsylvania. In all, hundreds of millions in new energy investment opportunities are available in the Commonwealth to help build a clean, indigenous, diversified energy industry in the state. This vision is creating excitement about Pennsylvania as an innovative, cutting-edge place to do business.

To build on this effort, Governor Rendell also enacted Act 178 of 2004, which provides \$10 million to the recently revitalized Pennsylvania Energy Development Authority to finance projects that develop, promote and more efficiently use alternative energy resources indigenous to the state. With resources administered by the Department of Community and Economic Development, the state has up to \$900 million to offer in tax-free bond financing for projects built in the Commonwealth.

CONTACT: Kate Philips, Pennsylvania Office of the Governor, +1-717-783-1116.

SOURCE Pennsylvania Office of the Governor